# POLITECNICO DI TORINO

Master of Science in Civil Engineering


## MASTER OF SCIENCE DISSERTATION

# A PARAMETRIC ANALYSIS FOR THE TORQUE AND BEARING CAPACITY CALCULATION OF HELICAL PILES IN COHESIONLESS SOILS

**Candidate:**

Carlos Mauricio Mendez Solarte

**Supervisor:**

Prof. Pierpaolo Oreste

Dr. Giovanni Spagnoli

Academic Year 2017-2018

# CONTENTS

# LIST OF SYMBOLS

$A_b$ bottom surface area of the screw blade ($m^2$)

$A_h$ projected helix area ($m^2$)

$A_t$ top surface area of the screw blade ($m^2$)

$a$ angular coefficient of the straight line

$D$ diameter of the screw anchor's blade (m)

$D_j$ diameter of helical plate (m)

$D_{h1}$ depth to helix 1 (m)

$D_{hj}$ depth to helix j (m)

$d$ diameter of the anchor's shaft (m)

$d_c$ diameter of a circle corresponding to the helix surface (m)

$F$ lateral force acting on the screw anchor's blade

$F_q$ breakout factor of the helix

$H$ length of the shear failure zone above helix (m)

$K_a$ coefficient of active earth pressure

$K_f$ coefficient of friction between the anchor's shaft and the soil

$K_P$ coefficient of passive earth pressure

$K'_p$ modified coefficient of passive earth pressure

$K_s$ coefficient of lateral earth pressure

$K_0$ coefficient of lateral earth pressure at rest

$K_t$ empirical torque factor

$L$ pile length in which shaft friction is considered (m)

$N_q$ bearing capacity factor

$F_q$ breakout factor for anchors

$P$ power (MW)

$p$ pitch of the screw pile (m)

$Q_h$ ultimate uplift capacity of a helix (MN)

$Q_s$ shaft resistance (MN)

$Q_u$ ultimate pull-out resistance of pile determined from ground base (MN)

$q_s$ average unit shaft friction of soil (kPa)

$r$ distance from the centre of the pile (m)

$T$ total value of installation torque (MNm)

$T_i$ torque (MNm)

$t$ thickness of the screw (m)

$U$ perimeter of pile (m)

$V$ vertical pushing down force (kN)

$V_i$ vertical force (kN)

$\sigma_{id,max}$ maximum ideal stress on the external ring of the pile at the surface (MPa)

$\sigma'_v$ effective vertical pressure ($kN/m^2$)

$\sigma'_{vj}$ effective vertical stress at the middle of helix ($kN/m^2$)

$\theta$ helix angle (°)

$d\theta$ infinitesimally angle in the polar coordinates (°).

$\delta$ angle of shearing resistance soil/pile (°)

$\delta_{cv}$ constant volume interface friction angle soil/pile (°)

$\phi$ friction angle the soil (°)

$\beta$ pull-out factor

$\gamma$ unit weight of the soil ($kN/m^3$)

$\psi$ helix angle of the helical-shaped screw unit (°)

# INTRODUCTION

Helical piles are light weight type of deep foundation systems and were first invented by Alexander Mitchell in 1836. The first application of helical-piles as a foundation for marine structures was for the Maplin Sands Lighthouse in 1838 (Lutenegger, 2011). Recent helical piles consist of one or more steely circular helical plates welded to a circular or square steel shaft at a specified spacing shaft diameter (Askari et al., 2016).

In the evolution of foundation piles, various construction methods have been developed and used at actual construction sites. However, in the relationship between pile construction and the environment, focus of attention has been on problems such as noise and vibration during construction, treatment of surplus soil, groundwater pollution, etc, (Chikawa and Kono, 2014).

The available research and design methodologies for helical anchors to date are relatively more limited than other conventional piling techniques (Mittal and Mukherjee 2013).

Helical (screw) piles are a valid form of foundations and they have been successfully used in different ground conditions including marine environments (Arup Geotechnics 2005; Spagnoli, 2013). They are installed in soil by applying a torque to the upper end of the shaft by mechanical means (Tsuha and Aoki, 2010). Helical piles are made by high strength steel strength and are composed of an open or closed end-pipe and a helix (or multiple helices) welded at the pipe end (Spagnoli, 2017).

These piles are classified as low displacement piles as the volume of soil displaced is relatively low (Weech et al. 2012). Several studies have been conducted on these types of pile, such as installation torque assessment (e.g. Ghaly and Hanna, 1991; Ghaly et al., 1991a; Perko, 2000; Tsuha, 2007; Spagnoli, 2017), estimation of the bearing capacity (e.g. Mitsch and Clemence 1985; Rao et al., 1991; Ghaly et al., 1991b; Mittal and Mukherjee, 2013; Gavin et al., 2014; Fateh et al., 2017), response to cyclic and lateral loads (e.g. Newgard et al., 2015; Al-Baghdadi et al., 2015; Schiavon et al., 2016; 2017). Helical piles are commonly used for resisting uplift forces due to the anchor effect of the helix (e.g. Saeki and Ohki 2000).

According to Tsuha and Aoki (2010), the uplift capacity of helical piles is controlled by the torsional resistance to the pile penetration measured during installation and the installation effort is used as a tool to evaluate foundation quality. Similarly, Livneh and Naggar (2008) state that the average installation torque is related to the compressive and uplift capacities. Kt value, which relates the uplift capacity to the torque required to install helical piles to the desired depth, is normally employed for assessing the correlation torque to uplift capacity (Hoyt and Clemence, 1989).

Several correlations have been reported regarding the aforementioned parameters (e.g. Zhang, 1999; Tsuha and Aoki, 2010; Bagheri and El Naggar, 2015; Sakr, 2014; 2015). The relation between torque and uplift capacity for helical piles is very important, as the installation of helical piles produces a radial displacement of soil.

However, predicting the uplift behavior of helical piles is very complex as determination of stress-strain parameters for the disturbed soil, to calculate pile displacement during pull-out is not an easy task (Mosquera et al., 2016). Assessing the torque value during the installation is not an easy operation neither. Theoretically, the screw pile penetrates while rotating with the simple equation by the pitch amount, i.e. elevation change per rotation (Basu and Prezzi, 2009):

$$\eta = tan^{-1}\left(\frac{\delta_z}{\delta_\theta}\right) \quad (1)$$

where $\delta_z$ and $\delta_\theta$ are the vertical and rotational (torsional) displacements of the drilling tool used in pile installation. η represents the ratio of the advancement (penetration) of the drilling tool into the ground and the rotation of the drilling tool (Fig. 1). Therefore, if the helical pile penetrates by the same amount of the pitch for each single rotation η should be 45. Lower values mean slower rate of penetration of the drilling tool into the ground during drilling (installation in dense sands), while higher values of imply easier drilling conditions (expected for installation in loose sands). However, since the soil is an elasto-plastic material, it is pushed upward to get the penetration force (Saeki and Ohki, 2000). The fundamental mechanisms by which helical piles develop resistance to load are described in a manner consistent with basic principles of soil mechanics (Perko, 2009).

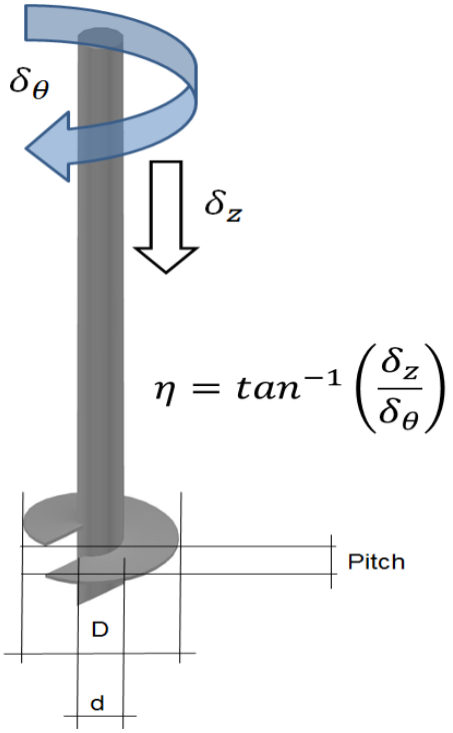


**Fig. 1 Schematic representation of the installation parameter for helical piles (adapted from Basu and Prezzi 2009).**

Torque calculation is needed also to assess the strength of the pile material, in order not to damage it (Spagnoli and Gavin, 2015). In addition, the calculation of the power required to install helical foundations is fundamental for the selection of the most appropriate equipment to guarantee a successful installation.

This thesis presents an estimation of the power needed to install helical piles in dry cohesionless soils under different conditions. For the estimation of installation power, three different theoretical models proposed to calculate the final installation torque of helical piles in non-cohesive soils were used (Ghaly and Hanna, 1991, Tsuha and Aoki, 2010 and Sakr, 2015). Additionally, a comparison between measured installation power of a helical pile installed in centrifuge by Schiavon (2016) and the theoretical results obtained using the torque models of Ghaly and Hanna (1991), Tsuha and Aoki (2010) and Sakr (2015) is presented. After that a parametric analysis has been conducted to observe which geotechnical and geometrical parameter influence the installation power of the helical pile.

For this investigation has been selected the offshore field, helical piles are being considered as novel offshore pile system, because of their flexibility regarding ease of installation and high large uplift capacity they can generate.

The offshore structures, both for oils and gas and renewable energies, driven piles are the most used foundation type (Poulos, 1988; Randolph and Gourvenec, 2011). These piles are often subjected to uplifting forces (e.g. Chattopadhyay and Pise, 1986; Das, 1989; Gavin et al., 2011; Jardine et al., 2015). Because of large tension capacity that can be developed by large-diameter helical piles (also known as screw piles), they can be employed as an alternative to driven steel tubular piles to support these structures (Spagnoli, 2017), also because they can be cost effective in providing tension resistance for foundation where the soil conditions permit the installation (Mitch and Clemence, 1985).

They are installed in soil by applying a torque by means of a hydraulic torque motor (Aydin et al., 2011; Spagnoli et al., 2015) to the upper end of the shaft and they should penetrate the soil in a smooth and continuous manner at a rate of rotation between 5 and 20 rpm (AB Chance Co., 2010). A small crowd force is applied during the installation to maintain advancement of the helical pile into the soil (Ghaly et al., 1991) theoretically at constant penetration rate equal to pitch size per full revolution (Perko, 2009). However, "*most of helical pile manufactures claim that crowd is a small component to the pile installation, and they recommend neglecting it*" (Sakr, 2015).

Helical piles are made by high steel strength and are composed of an open or closed end-pipe and a helix welded at the pipe end (single helix), multiple-helices are also common (multi-helix) and there are also piles with a continuous helical wing fixed around a pipe shaft (continuous helix) (e.g. Nagata and Hirata, 2005; Spagnoli, 2017; Wada et al., 2017).

Generally helical piles are known to be of small diameter-up to 269mm shaft diameter (Perko, 2009) and they are normally employed for foundations for transmission towers, as a support for excavation shoring during shotcrete applications, to support mezzanines or additional floors in existing buildings.

For large structures, helical piles are very common in Japan or in general in Asian countries, where piles with shaft diameters up to 1600mm with helix-to-shaft ratios up to 2.5 (e.g. Mori, 2003; Saeki and Ohki, 2003; Nagata and Hirata, 2005; Sakr, 2009) are

employed as foundation systems for bridges, buildings, to resist seismic loads and for general civil engineering works (Fig. 2).

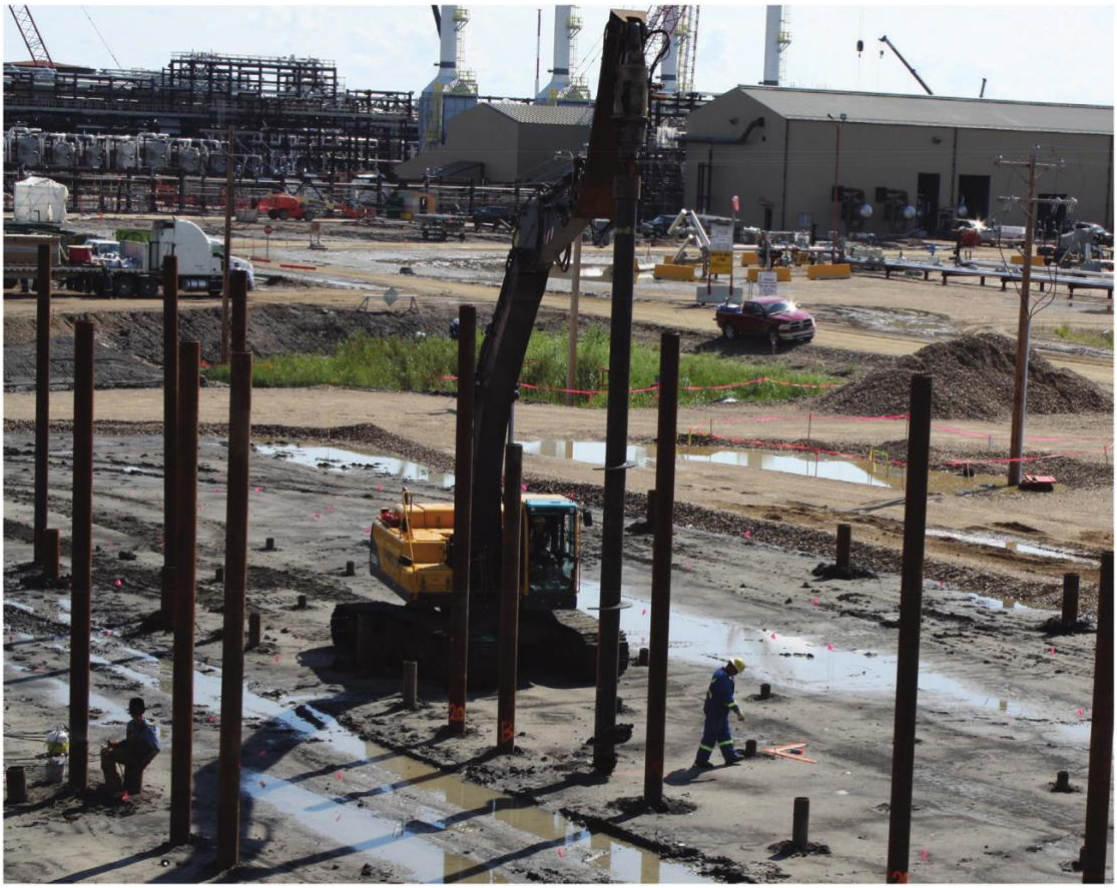

**Fig. 2 Typical helical pile installation (from Sakr, 2015).**

Helical piles have been suggested as a potential alternative to driven piles as offshore pile (e.g. Spagnoli, 2013; Spagnoli and Gavin, 2015; Spagnoli et al., 2015; Al-Baghdadi et al., 2015; Byrne and Houlsby, 2015; Fateh et al., 2017), because they provide a large uplift capacity due to the anchor effect of the helix, they do not produce any backflow, muddy water, or waste materials at all, they have excellent deformation capacity, strength, and seismic performance (Saeki and Ohki, 2000). In the offshore environment, high axial pile capacity is needed. Typical values range from 6MN for a wind turbine with a capacity of 3.5MW (Byrne and Houlsby, 2003), to up to 40MN for oils and gas fixed platforms (e.g. Kraft and Lyons, 1974; De Mello et al., 1983). In order to achieve the requested axial pile capacity large embedment depths are required (see Young and Sullivan, 1978). Helical piles are not common, in offshore environment, though.

Because few data are available for possible applications of offshore screw piles, this research tries to assess the uplift capacity of three helical piles with different wing ratios, i.e. helix-to-shaft ratio (1.5, 2.0 and 2.5) with a shaft diameter of 500mm in a sand with varying friction angle values, to simulate different density conditions (e.g. Peck et al., 1974), and the corresponding installation power is calculated by estimating the torque values according to the model of Tsuha and Aoki (2010).

# 1. METHODOLOGY FOR THE BEHAVIOR ANALYSIS OF THE PILES DURING THE INSTALLATION

The models of Ghaly and Hanna (1991), Tsuha and Aoki (2010) and Sakr (2015) have been used because they are easily comparable among each other. Besides, the input parameters can also be adjusted to employ them for real in situ tests. Even though the methods are easily comparable among each other, they also analyze the parameters from several points of view because each of these methods were evaluated under different conditions. Ghaly and Hanna method was verified using laboratory tests on a dry sand, the Sakr (2015) method was compared with field results and the Tsuha and Aoki method, that relates the installation torque to the pile capacity, was validated using centrifuge model tests. The theoretical model assumes that the exerted torque during helical pile installation into sandy soils is resisted by frictional and bearing resistances of pile shaft and helices (Sakr, 2015). Summation of moments due to frictional resistances acting on the surface area of the helices and shaft yields the moment required to overcome the resisting soil moments during installation (i.e. installation torque) (Sakr, 2015).

## THEORETICAL MODEL OF GHALY AND HANNA (1991)

Ghaly and Hanna (1991) conducted some lab tests in dry sand with different density states to assess the geometrical parameters on the installation. Torque values (among other parameters such as pull-out, upward displacement, stress development) were recorded. The factors influencing the installation and the theoretical installation model were obtained.

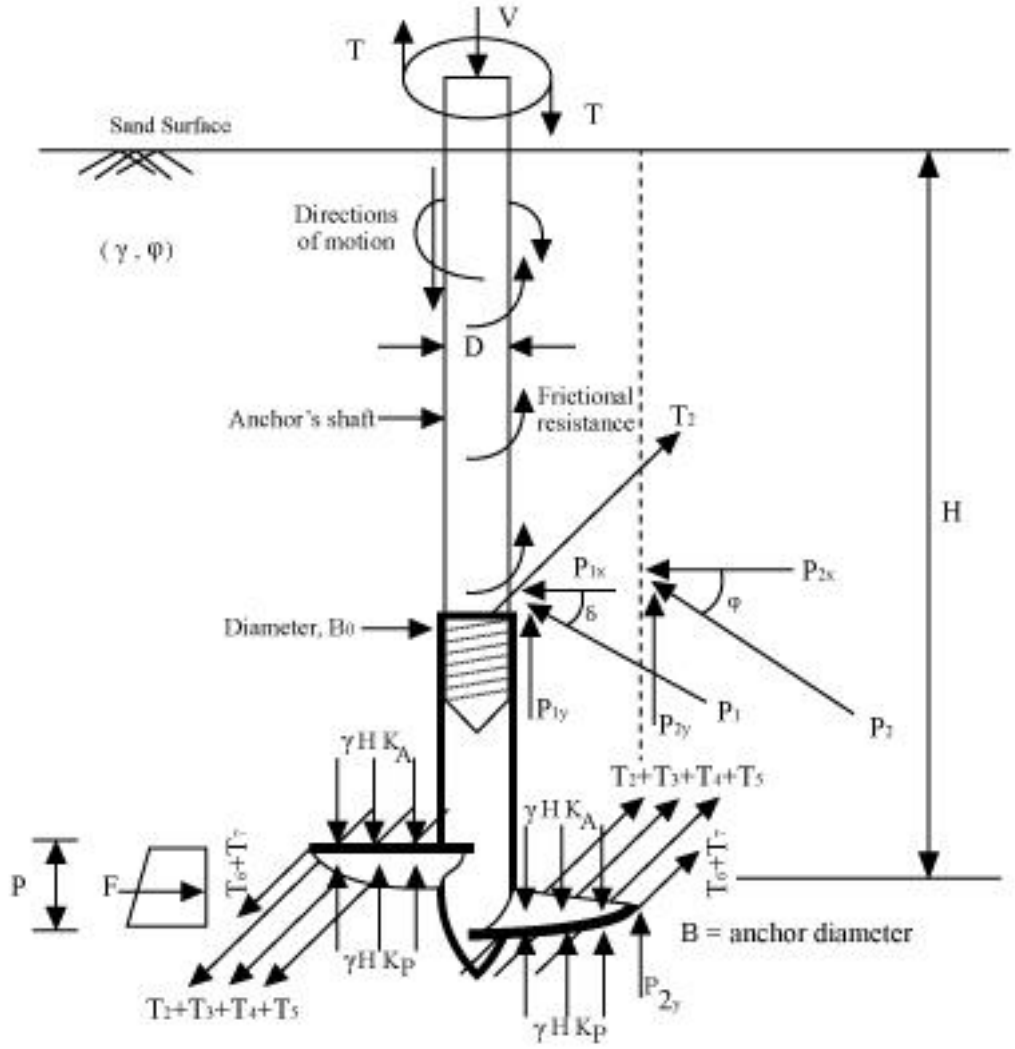


**Fig. 3 Forces acting on single pitch screw anchor during installation (from Ghaly and Hanna, 1991).**

The figure 3 shows the forces and torques acting on a single pitch screw pile as set out by Ghaly and Hanna, (1991) and the equations stablished in this theoretical model are the following:

$$T = \sum_{i=1}^{n} T_i \quad (2)$$

The resisting moment acting $T_1$ on the anchor's shaft owing to the force $P_{1x}$:

$$T_1 = 0.5\gamma H^2 \cos(\delta) K'_p K_f (\pi d)(d/2) \quad (3)$$

The resisting moment acting $T_2$ on the anchor's blade owing to the force $P_{1y}$:

$$T_2 = 0.5\gamma H^2 \sin(\delta) K'_p \tan(\delta + \psi)(\pi d)(d/2) \quad (4)$$

The resisting moment acting $T_3$ on the anchor's blade owing to the force $P_{2y}$:

$$T_3 = 0.5\gamma H^2 \sin(\delta) K'_p \tan(\delta + \psi)(\pi D)(D/2) \quad (5)$$

The resisting moment acting $T_4$ on the upper surface of the anchor's blade owing to the acting active earth pressure which develops as a result of the downward movement of the anchor' blade away from the overlying sand mass:

$$T_4 = \gamma H K_a A_t \tan(\delta + \psi)[(D + d)/4] \quad (6)$$

The resisting moment acting $T_5$ on the lower surface of the anchor's blade owing to the acting passive earth pressure which develops as a result of the applied pushing-down force:

$$T_5 = \gamma H K_p A_b \tan(\delta + \psi)[(D + d)/4] \quad (7)$$

The resisting moment $T_6$ owing to the bearing force F acting on the entire height of the screw pitch:

$$T_6 = F[(D - d)^2/8] \; ; \; F = 0.5\gamma H K_p (1 + p)p \quad (8)$$

The resisting moment acting $T_7$ on the outer perimeter of the thickness of the screw blade:

$$T_7 = \gamma H K_p K_f (\pi D)(D/2)t \quad (9)$$

## THEORETICAL MODEL OF TSUHA AND AOKI (2010)

Tsuha and Aoki (2010) presented a relationship between uplift capacity and installation torque for deep helical piles in sand. Centrifuge and direct shear interface tests, were carried out with dry Fontainebleau sand samples to evaluate the proposed theoretical relationship. The equation and scheme stablished in this model are the following:

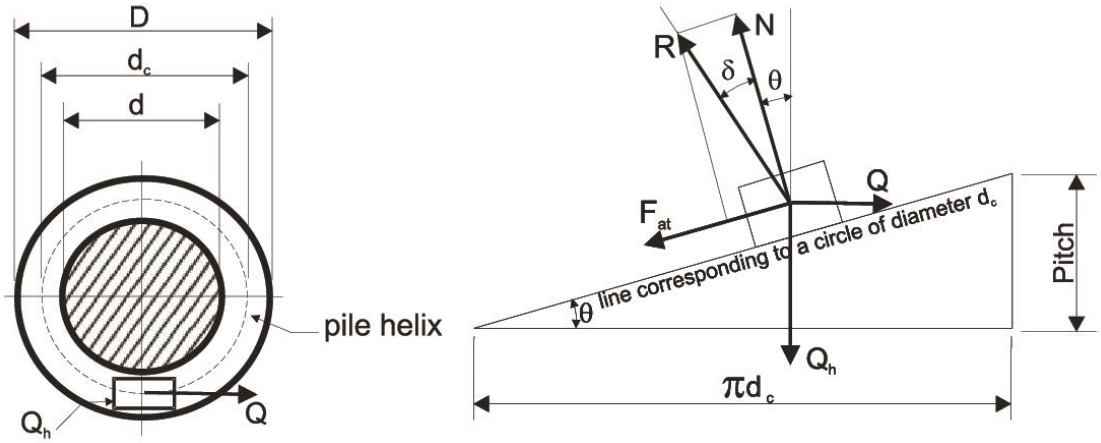


**Fig. 4 Top view of the pile helix and the surface during helical pile installation in sand (from Tsuha and Aoki, 2010).**

$$T = \frac{Q_s d}{2} + \frac{\sum_{i=1}^{N} Q_h d_c \tan(\theta+\delta)}{2} \quad (10)$$

Where $d_c$ is the diameter of a circle corresponding to the surface area of helix, $\theta$ is the helix angle with the horizontal at $d_c$, and $\delta$ is the residual interface friction angle between helix material and surrounding sand at the depth of the helix (when the pile penetrates sand layers of differing characteristics). The use of equation (10) is a simplified method to determine the final installation torque to control on site the uplift capacity of deep helical piles in sand. (Fig. 4) (Tsuha and Aoki, 2010).

The diameter of a circle corresponding to the helix sur- face area $d_c$ and helix angle $\theta$ can be given by the following expressions:

$$d_c = \frac{2}{3}\left(\frac{D^3-d^3}{D^2-d^2}\right) \quad (11)$$

$$\theta = \tan^{-1}\left(\frac{p}{\pi d_c}\right) \quad (12)$$

Where $p$ is the helix pitch.

The shaft resistance $Q_S$ can be estimated from the following expression (CFEM 2006):

$$Q_s = \pi d L q_s \quad (13)$$

Where $d$ is the shaft diameter, $L$ is the length of pile shaft and $q_s$ is the average unit shaft friction of soil (Sakr, 2015).

The average unit shaft friction for the cohesionless soils can be estimated using the following expression:

$$q_s = \sigma'_v K_s \tan(\delta) \quad (14)$$

Where $\sigma'_v$ is the effective vertical stress at the mid depth of the pile, $K_s$ is the coefficient of lateral earth pressure and $\delta$ is the interface friction angles (Sakr, 2015).

The ultimate uplift capacity $Q_h$ of the helix can be estimated from the following expression (Das, 1990):

$$Q_h = A_h(\gamma D_{hj} F_q) \quad (15)$$

Where $A$ is the projected helix area of a helix $j$, $\gamma$ is the average unit weight of the soil to helix $j$ depth, $D_{hj}$ is the depth to a helix $j$ and $F_q$ is the breakout factor of a helix $j$ (Das 1990) (Sakr, 2015).

The breakout factor for anchors, $F_q$, for embedment depths smaller than 10D can be estimated using the chart of Vesic (1971) for circular shallow anchors. A comparison between different theories presented in Das (2002) shows that Vesic theory gives more conservative values of $F_q$, and as the helical pile installation disturbs the soil above the helix, this theory was used in the current investigation. Additionally, Vesic's values showed good agreement with the measured results of $F_q$ obtained in Schiavon (2016) for helical anchors installed at embedment depth of $7.4D$ ($D$ is helix diameter) in very dense sand.

However, as the breakout factor becomes constant after a critical embedment depth (for greater embedment depths, a local shear failure in soil located around the anchor takes place), in the current work, for embedment depths greater than $10D$, we used the values of $F_q$ proposed in the A.B. Chance Co. (2010). They recommend lower values of $F_q$ to reproduce the performance of helical anchors influenced by the soil disturbance caused by pile installation.

## THEORETICAL MODEL OF SAKR (2015)

Sakr (2015) proposed a theoretical model developed to estimate the torsional resistance of cohesionless soils to helical pile installation. The theoretical torque model was verified using installation records collected from different sites. The equations stablished in this theoretical model are the following:

$$T = T_1 + \sum_{j=1}^{N} T_{2j} + T_{3j} + T_{4j} + T_{5j} + T_{6j} + T_{7j} + T_{8j} \quad (16)$$

Where $N$ is the number of helices; $T_1$ is the torsional moment acting on the pile shaft (kN·m); and $T_{2j}$–$T_{8j}$ are the torsional moment components acting on a helix $j$ (kN·m) (Fig. 5). Forces resisting installation of helical piles by rotation can be listed following a similar model to that developed by Ghaly and Hanna (1991) (Sakr, 2015).

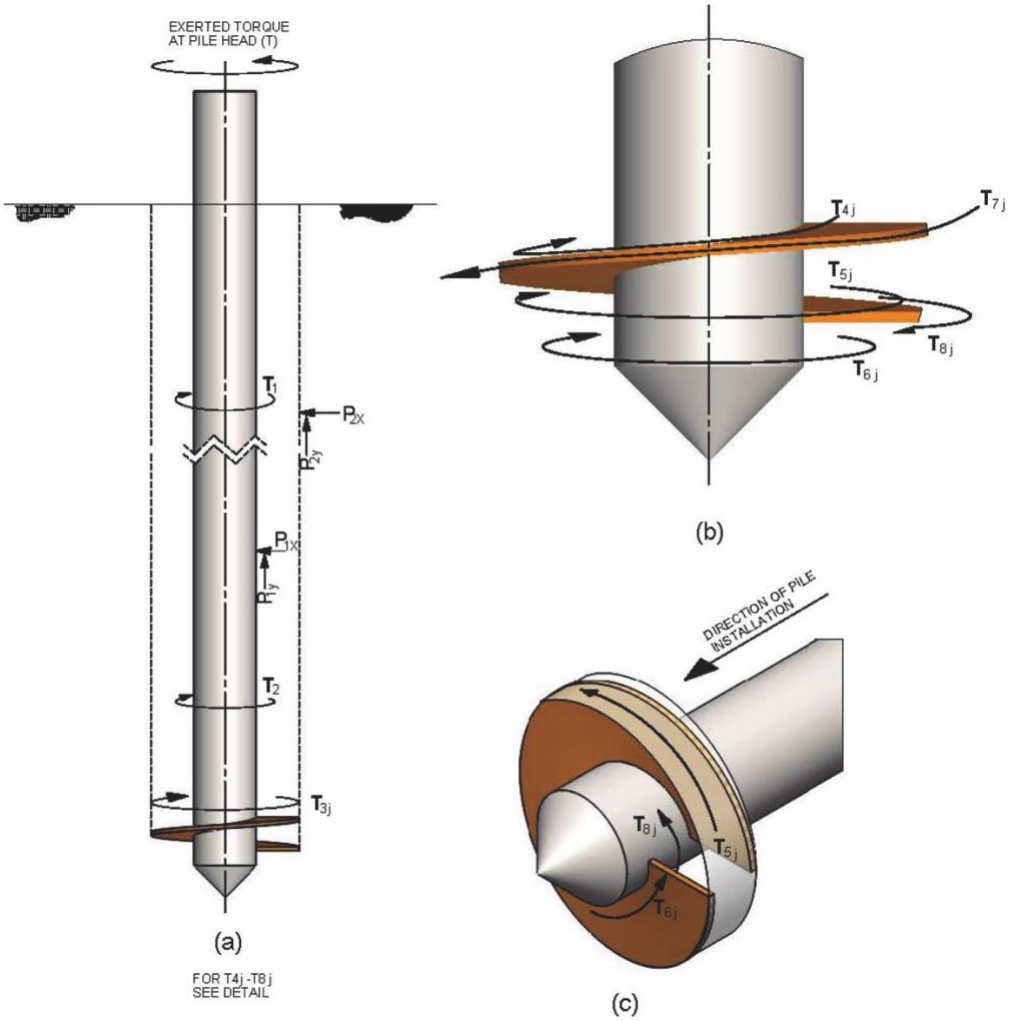


**Fig. 5 Proposed theoretical torque model: (*a*) overall resisting moments; (*b*) resisting moments at helix level; (*c*) isometric view. $P_{1x}$, $P_{1y}$, $P_{2x}$, $P_{2y}$, passive lateral earth pressure components; $T_1$, $T_2$, $T_{3j}$–$T_{8j}$, torsional moment components (from Sakr, 2015).**

Passive lateral earth pressure exerted on the pile shaft ($P_1$). As shown in Fig. 5, force $P_1$ has two components, $P_{1x}$ and $P_{1y}$: $P_{1x}$ produces moment acting on the shaft ($T_1$), and $P_{1y}$ produces moment acting on the helix ($T_{2j}$) (Sakr, 2015).

$$T_1 = \sigma'_v D_{h1} \cos(\delta) K_p K_f \frac{\pi d^2}{4} \quad (17)$$

$$T_{2j} = \sigma'_{vj} (D_{hj} - D_{h(j-1)}) \sin(\delta) K_p \tan(\delta + \psi) \frac{\pi d^2}{4} \quad (18)$$

Where $\sigma'_v$ is he average effective vertical stress along the pile shaft, $D_{h1}$ is the depth to helix 1 (the upper helix), $\sigma'_{vj}$ is the effective vertical stress at the middle of helix $j$, $D_{hj}$ is the depth to helix $j$, $K_p$ is the coefficient of passive earth pressure, $K_f$ is the coefficient of friction between the pile shaft material and soil, $\delta$ is the interface friction angle between the pile material and, $\psi$ is the pitch angle, $p$ is the helix pitch, $D$ is the helix diameter and $d$ is the pile shaft diameter (Sakr, 2015).

The resisting moment acting on the helix ($T_{3j}$) owing to the force $P_{2y}$ acting on the outer side of the helix $j$ perimeter:

$$T_{3j} = \sigma'_{vj} (D_{hj} - D_{h(j-1)}) \sin(\delta) K_p \tan(\delta + \psi) \frac{\pi D^2}{4} \quad (19)$$

The resisting moment acting on the upper surface of the helix owing to the active earth pressure, $K_a$ ($T_{4j}$):

$$T_{4j} = \sigma'_{vj} K_a \tan(\delta + \psi) \frac{\pi (D^3 - d^3)}{12} \quad (20)$$

The resisting moment acting on the lower surface of the helix owing to the passive earth pressure ($T_{5j}$):

$$T_{5j} = \sigma'_{vj} K_p \tan(\delta + \psi) \frac{\pi (D^3 - d^3)}{12} \quad (21)$$

The resisting moment along the circumference of the helix $j$ ($T_{6j}$):

$$T_{6j} = \sigma'_{vj} K_p p \tan(\phi) \frac{\pi (D^2)}{2} \quad (22)$$

The resisting moment acting on the side surface of outer perimeter of the helix $j$ ($T_{7j}$):

$$T_{7j} = \sigma'_{vj} K_p t_j K_f \frac{\pi (D^2)}{2} \quad (23)$$

where $t_j$ is the thickness of helix $j$.

Moment due to leading edge penetrating into soil ($T_{8j}$):

$$T_{8j} = (D - d)N_q t_j \sigma'_{vj} \frac{(D+d)}{4} \quad (24)$$

It can be seen from Equations [17] to [24] that there are numerous factors that affect resisting moments to helical pile installation (or installation torque) including pile configuration and soil properties. Unlike the Tsuha and Ghaly model, Sakr considers the bearing capacity factor of Terzaghi, $N_q$, for obtaining the torque value. This factor depends from the mechanical properties of the soil and installation method of the pile (Colombo and Colleselli 1996).

## COMPARISON OF THE THEORETICAL MODELS

It can be observed that the forces resisting installation of helical piles by rotation given by Sakr (2015) are similar to the model by Ghaly and Hanna (1991). However, Sakr utilizes the effective stresses approach while Ghaly and Hanna model is based on total stresses approach. This difference is critical specially for full scale piles where embedment depth is deep and where groundwater level is relatively high (Sakr, 2015). For the comparisons in this paper, dry sand has been assumed so that the forces for Ghaly and Hanna are also considered effective. Another important difference between these two models is that Ghaly and Hanna (1991) recommended a reduced coefficient of passive earth pressure ($K_{p'} = 0.3\ K_p$), and Sakr (2015) suggested the use of a typical coefficient of passive earth pressure ($K_p = (1 + \sin\phi) / (1 - \sin\phi)$). As consequence, the results of the parametric analysis presented here shows that the results of power estimated using the torque model of Sakr (2015) are much higher than those obtained using Ghaly and Hanna's model.

The installation torque estimated using the model proposed in Tsuha and Aoki (2010) is dependent on the helix bearing resistance, shaft resistance, and the frictional resistance at the helix interface with the sand mass during installation. For this case, the soil parameters used for the other two models mentioned above are not necessary.

## INSTALLATION POWER

In this manuscript, the comparison among the models is performed in terms of power (P) calculation (in kW) rather than torque. P is the energy developed in the unit of time.

P is an interesting parameter because it permits to know the specifications required of the machine to install a pile in a soil with different geotechnical properties. The values of power are given by following equation:

$$P = P(T) + P\ (V) = \ T\omega + V\frac{\omega}{2\pi}p \tag{25}$$

$$v = \frac{\omega}{2\pi}p \tag{26}$$

Among the works mentioned above, only Ghaly and Hanna (1991) presented an equation to estimate the magnitude of the downward vertical force ($V$) required to overcome the forces acting against the downward motion. Therefore, to estimate the installation power in the current paper, the crowd force applied on the pile during installation (to maintain advancement of the helical pile into the soil at constant penetration rate equal to pitch size per full revolution) can be given by the following equations (Ghaly and Hanna 1991):

$$V = \sum_{i=1}^{n} V_i \tag{27}$$

The vertical force $V_1$ is the component $P_{1y}$ of the force $P_1$ acting on the anchor's shaft:

$$V_1 = 0.5\gamma H^2 \sin(\delta) K'_p(\pi D) \tag{28}$$

The vertical force $V_2$ is the component $P_{2y}$ of the force $P_2$ acting on the sand column overlying the anchor's blade:

$$V_2 = 0.5\gamma H^2 \sin(\phi) K'_p(\pi B) \tag{29}$$

The vertical force $V_3$ is the resulting from the passive bearing resistance acting on the lower surface of the screw blade:

$$V_3 = \gamma H K_p A_b \cos(\psi) \tag{30}$$

The vertical force $V_4$ is the drag force acting on the upper surface of the screw blade owing to the acting active earth pressure:

$$V_4 = \gamma H K_a A_t \cos(\psi) \tag{31}$$

Substituting the value of $V_1$, $V_2$, $V_3$ and $V_4$ in the equation (27), the magnitude of the downward vertical force $V$ can be determined (Fig. 3) (Ghaly and Hanna, 1991).

# 2. COMPARISON OF THE METHODOLOGY BEHAVIOR ANALYSIS AND THE ON-SITE MEASUREMENTS

## INSTALLATION DATA OF SCHIAVON ET AL. (2017)

To assess the validity of the three theoretical models, first the equations were compared to their respective models, to see whether they provided the same results as obtained in their respective researches. After this, they have been applied to the centrifuge model tests performed by Schiavon et al. (2017) on eight piles in a very dense sandy soil. The complete installation data is available in the thesis of Schiavon (2016) and they are shown in Fig. 6. The piles had a helix diameter, D, of 0.33m, shaft diameter, d, of 0.1m, and a pitch of 0.097m, which is 1/3 of D. The main geotechnical properties of the sand are listed in the paper of Schiavon et al. (2007) and for the models the most important are:

Average sand dry density of 1.55 g/cm$^3$;

peak friction angle, obtained by triaxial and direct shear tests of 47.5°;

The pile/soil interface friction angle, $\delta$, values have been assumed as 29°, which is the critical interface pile/soil friction angle, $\delta_{cv}$,based on the grain size distribution of the sand and particularly on the $D_{50}$ value, adapted from the ICP-05 guidelines (Lehane et al. 2005). In the tests performed by Schiavon et al. (2017), the sand used was very fine with $D_{50}$= 0.12, which corresponds to 29°. The usage of the $\delta_{cv}$ seems to be the most appropriate frictional parameter for piles in sand and does not depend on the relative density of the soil (Jardine et al., 1993).

The piles were installed at a depth of 7.4D (i.e. 2.44m) with a rpm value of 5.3, which corresponded to the penetration of one pitch per revolution.

After the evaluation of the three models using experimental data, a parametric analysis has been finally carried out for different friction angle and unit weight values of the sand, with D/d ratio of 1.5 and 2, with different rpm and blade thickness values. Besides the impact of the wing ratio, i.e. D/d, on the power installation value for a dense sand at 10m depth with constant assumed geotechnical properties has been assessed.

## RESULTS AND DISCUSSIONS

### Comparison between measured and theoretical results

The eight piles with the geometrical characteristics shown above have been installed in the same sand type. The installation data are (torque, downward force and power) are shown in Fig. 6, and the x-axis shows the ratio between the depth of the helix (during installation) and the helix diameter (0.33mm).

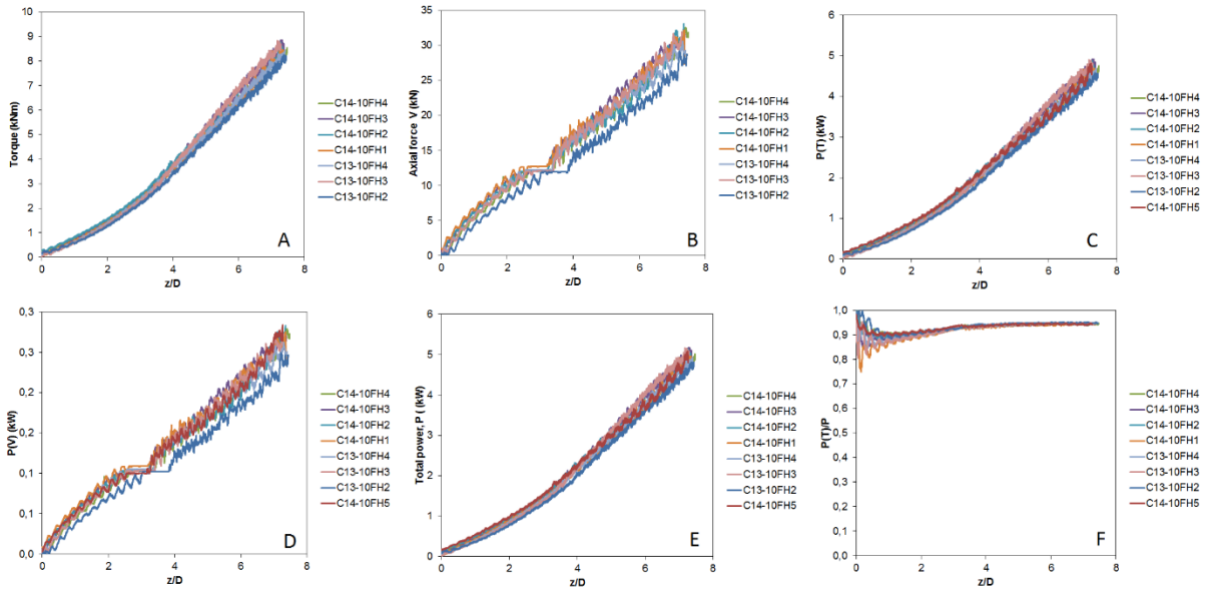


**Fig. 6 Installation power values for the 8 screw piles installed by Schiavon et al. (2007) vs depth normalized by D. A show the torque value, B the axial force, C the power from the torque, D the power from the axial force, E the total power and F the power from the torque divided by the total power (from Spagnoli et al. in review).**

From Fig. 6 is possible to observe that:

the total power values are very similar for the 8 piles;

during installation, after a penetration of around 4D, the values of torque power, P(T), is around 95% of the total power (only 5% of power is related to the vertical downward force);

before a depth of 4D (beginning of installation) the values of power related to the downward vertical force, P(V), varied from 0 to 20% (and is more variable);

the most important fraction of installation power is related to the installation torque. This finding agrees with field observations. As cited in Sakr (2015), most of helical pile

manufactures claim that crowd is a small component to the pile installation, and they recommend neglecting it.

Fig. 7 shows the comparison for the experimental installation torque and power values for Schiavon et al. (2017), vs the three models. For the theoretical predictions, an interface soil/pile critical angle, $\delta_{cv}$, of 29° as recommended in Lehane et al. (2005) has been chosen. The theoretical values based on the Sakr model (2015) overestimate the experimental results of installation torque and power. The other two models provided good agreement with the measured results. When comparing the final installation torque results, the model of Tsuha and Aoki (2010) showed better agreement. However, for lower depths (beginning of installation), this model underestimate the installation torque and power, and as the pile advances into the soil the predicted results become closer to the measured ones. It occurs probably because Tsuha and Aoki (2010) model was proposed for deep helical anchors (local shear failure in soil will take place at ultimate load).

The model of Sakr (2015) tends to overestimate torque and in turn power by 5 (at the beginning of the installation) to 20 times (at the end of the installation).

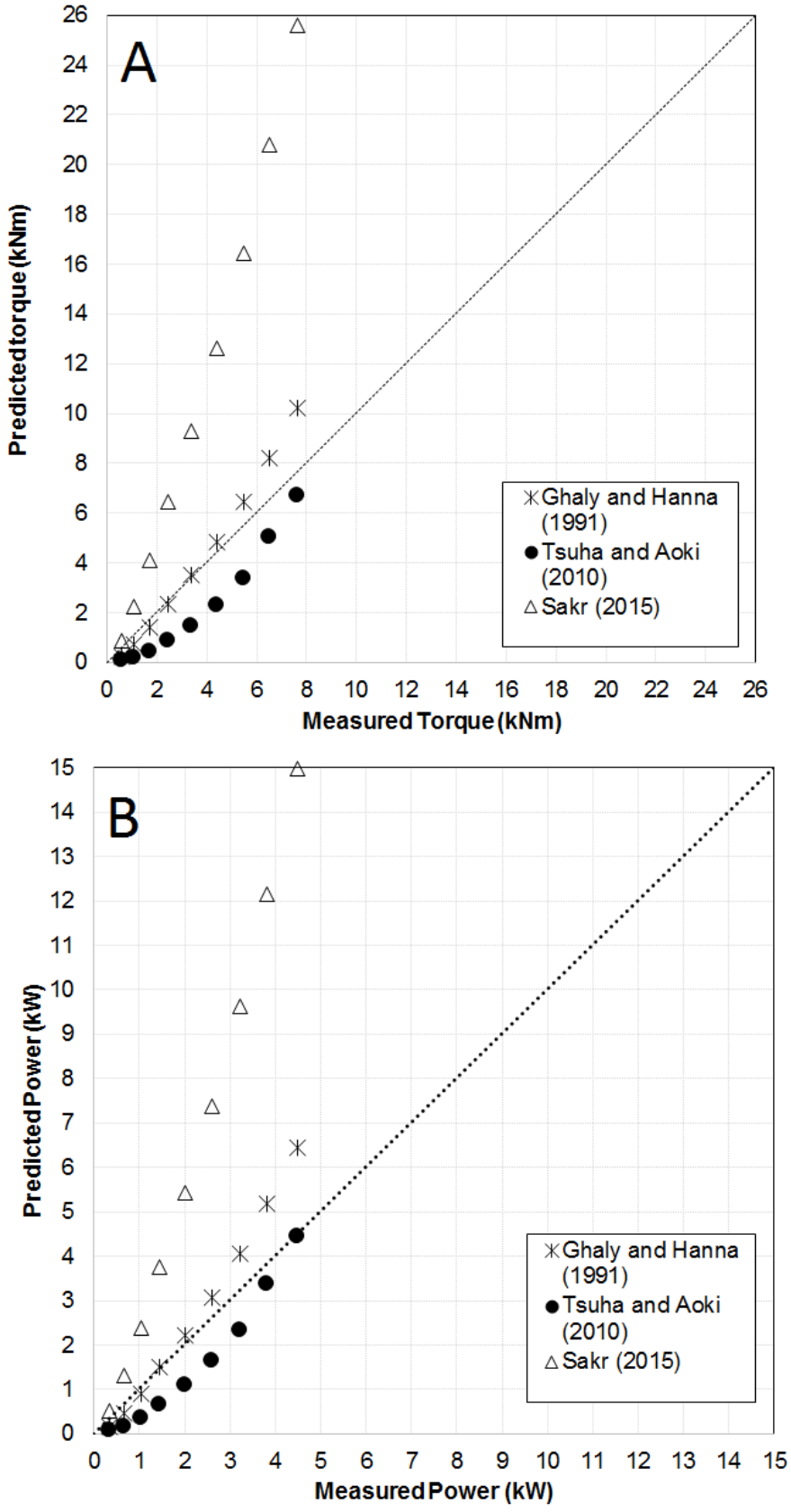


**Fig. 7 Experimental vs theoretical (A) installation torque and (B) installation power results (from Spagnoli et al. in review).**

# 3. PARAMETRIC ANALYSIS

For the parametric analysis two different approaches have been followed. Firstly, a single-helix helical pile with two fixed D-to-d ratios, here referred as wing ratio (D is 0.6m and d is 0.3 m with a pitch, p, of 1/3 of D and then D is 0.45 m and d is 0.3 m with a pitch 1/3 of D) has been compared with the three models by simulating a maximum depth of 10m in a sandy soil with varying unit weight volume, γ, from 13 to 22 kN/ $m^3$ as according to Lambe and Withman (1969) - varying friction angles, φ, from 29° to 41° to simulate loose, medium and dense state (Peck et al. 1974; Minnesota Department of Transportation 2007), with different rounds per minute, RPM, installation velocity values from 5 to 20 as described by A.B. Chance Co. (2010). As interface friction angle values, we used the critical interface friction angle value, $\delta_{cv}$ of 29° suggested in Lehane et al. (2005) for fine sand-steel interfaces. The critical interface friction angle is more appropriate to simulate the helical pile installation (under motion condition and large relative displacements). For the $F_q$ values we used the chart of Vesic (1971) for shallow embedment depths (< 10D) and for deep embedment depths (>10D) the chart of A.B. Chance Co. (2010). The reasons of using these values of $F_q$ are described previously in this paper.

Secondly, for a given set of data, i.e. φ (41°), γ (22 kN/$m^3$), RPM (20), blade thickness (25.4mm), the wing ratio has been varied (by increasing D and keeping constant d and viceversa). When D was constant, the pitch, remained also constant. When d was constant, the pitch varied with changing D values following the relation p= 1/3 D.

Considering the large number of parameters, it is not possible to show every single diagram. Therefore, just a couple of graphical examples have considered, and in Tab. 1 and 2 the results for the different parameters in a depth of 10m are listed.

Fig. 8 and 9 shows a comparison for a sand with the unit weight γ of 13 kN/$m^3$, and installation RPM of 5, for different soil friction angle values φ for a pile wing ratio of 2. As expected the larger depth causes larger P values, however the while the models of Ghaly and Hanna (1991) and Tsuha and Aoki (2010) deliver quite similar P values, despite the fact that the model of Ghaly and Hanna (1991) delivers P values up to 1.6 times the model of Tsuha and Aoki (2010). The model of Sakr (2015) gives P values

twice larger with respect to Ghaly and Hanna and five times larger considering the model of Tsuha and Aoki (2010).

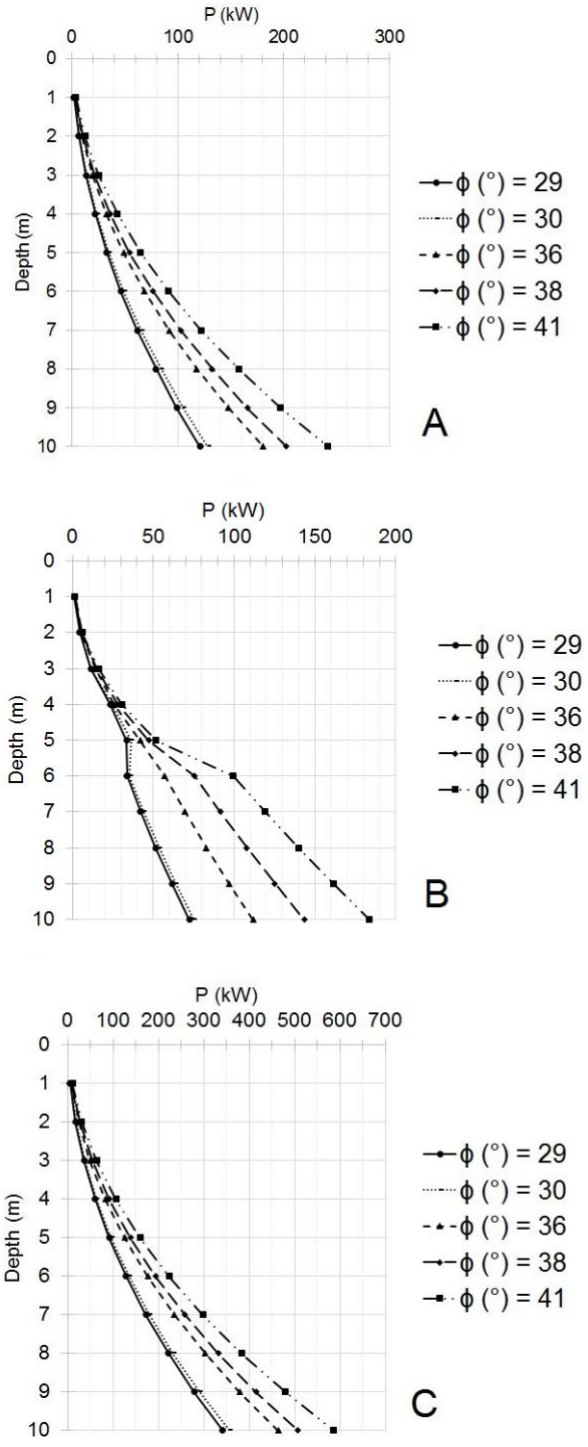


**Fig. 8 Model comparison of Ghaly and Hanna (1991) A, Tsuha and Aoki (2010) B and Sakr (2015) C for a sand with γ 13 kN/m$^3$, RPM 5 for different φ values for a D/d ratio of 2 (from Spagnoli et al. in review).**

Reducing the wing ratio to 1.5 and keeping constant the physical properties of the sand, the P values reduce of about 30 to 40% for all the models.

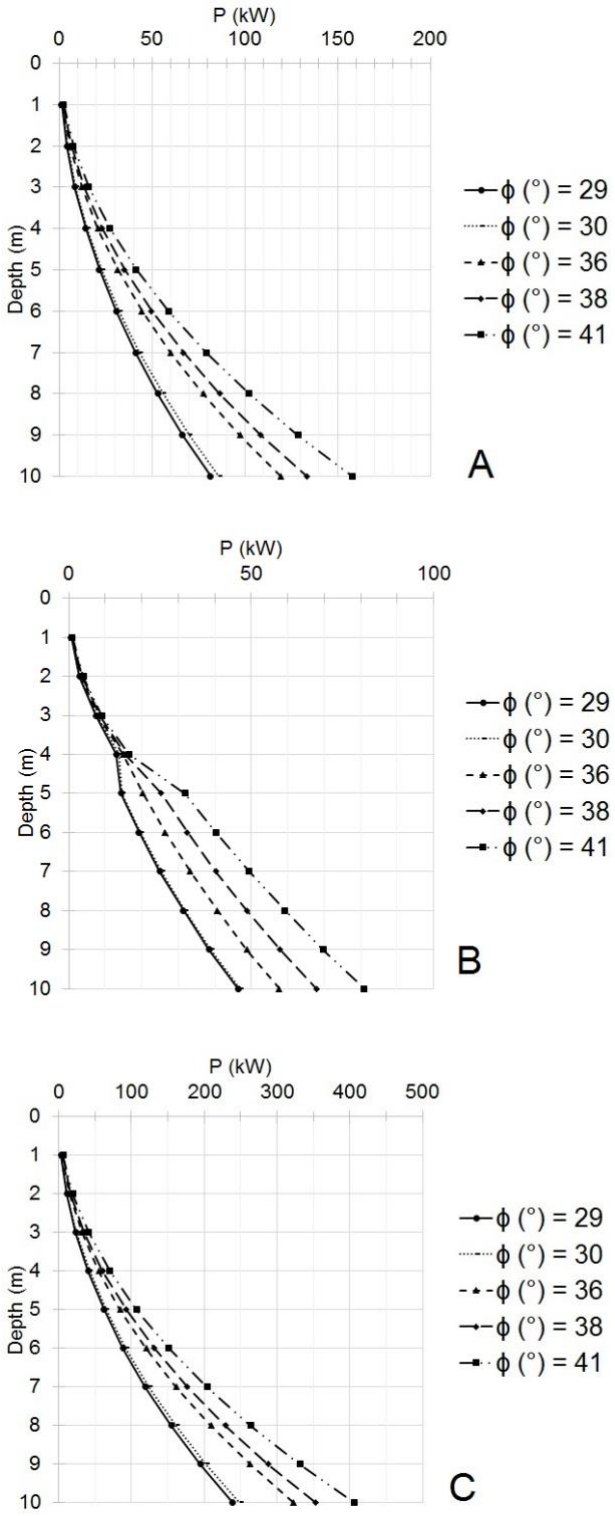


**Fig. 9 Model comparison of Ghaly and Hanna (1991) A, Tsuha and Aoki (2010) B and Sakr (2015) C for a sand with γ 13 kN/m$^3$, RPM 5 for different φ values for a D/d ratio of 1.5 (from Spagnoli et al. in review).**

Considering the large number of parameters interacting with each other, the results of the installation power values are shown in Tab. 1 and 2 for wing ratios of 1.5 and 2.

It is possible to state:

- For all three models the power increases with increasing unit weight of soil, friction angle of soil and increasing RPM values;
- Increasing the wing ratio from 1.5 to 2 the power increases of about 40%.

| **Power at 10 m and with D=2(d)** | | | **Ghaly and Hanna** | | | | **Mohammed Sakr** | | | | **Cristina da Hollanda** | | | |
|---|---|---|---|---|---|---|---|---|---|---|---|---|---|---|
| | | | **γ (kN/m^3)** | | | | **γ (kN/m^3)** | | | | **γ (kN/m^3)** | | | |
| | | | **13** | **16** | **19** | **22** | **13** | **16** | **19** | **22** | **13** | **16** | **19** | **22** |
| **5 rpm** | **φ (°)** | 29 | 121.1 | 149.1 | 177.0 | 205.0 | 341.3 | 420.0 | 498.8 | 577.5 | 72.4 | 89.1 | 105.9 | 122.6 |
| | | 30 | 128.2 | 157.8 | 187.4 | 217.0 | 356.1 | 438.3 | 520.5 | 602.6 | 75.0 | 92.3 | 109.6 | 126.9 |
| | | 36 | 180.7 | 222.3 | 264.0 | 305.7 | 464.9 | 572.2 | 679.4 | 786.7 | 112.0 | 137.8 | 163.7 | 189.5 |
| | | 38 | 202.7 | 249.5 | 296.3 | 343.1 | 510.6 | 628.5 | 746.3 | 864.1 | 143.4 | 176.5 | 209.6 | 242.7 |
| | | 41 | 241.5 | 297.3 | 353.0 | 408.8 | 591.2 | 727.7 | 864.1 | 1000.5 | 183.8 | 226.2 | 268.6 | 311.0 |
| **10 rpm** | **φ (°)** | 29 | 242.2 | 298.1 | 354.0 | 409.9 | 682.5 | 840.0 | 997.5 | 1155.0 | 144.9 | 178.3 | 211.7 | 245.1 |
| | | 30 | 256.4 | 315.6 | 374.8 | 433.9 | 712.2 | 876.6 | 1040.9 | 1205.3 | 150.0 | 184.6 | 219.2 | 253.9 |
| | | 36 | 361.3 | 444.7 | 528.1 | 611.4 | 929.8 | 1144.3 | 1358.9 | 1573.5 | 224.0 | 275.7 | 327.3 | 379.0 |
| | | 38 | 405.5 | 499.1 | 592.6 | 686.2 | 1021.2 | 1256.9 | 1492.6 | 1728.3 | 286.8 | 353.0 | 419.2 | 485.4 |
| | | 41 | 483.1 | 594.6 | 706.0 | 817.5 | 1182.4 | 1455.3 | 1728.2 | 2001.0 | 367.5 | 452.3 | 537.2 | 622.0 |
| **15 rpm** | **φ (°)** | 29 | 363.3 | 447.2 | 531.0 | 614.9 | 1023.8 | 1260.0 | 1496.3 | 1732.5 | 217.3 | 267.4 | 317.6 | 367.7 |
| | | 30 | 384.6 | 473.4 | 562.2 | 650.9 | 1068.3 | 1314.8 | 1561.4 | 1807.9 | 225.0 | 276.9 | 328.9 | 380.8 |
| | | 36 | 542.0 | 667.0 | 792.1 | 917.1 | 1394.7 | 1716.5 | 2038.3 | 2360.2 | 336.0 | 413.5 | 491.0 | 568.5 |
| | | 38 | 608.2 | 748.6 | 889.0 | 1029.3 | 1531.9 | 1885.4 | 2238.9 | 2592.4 | 430.2 | 529.5 | 628.8 | 728.1 |
| | | 41 | 724.6 | 891.8 | 1059.1 | 1226.3 | 1773.6 | 2183.0 | 2592.3 | 3001.6 | 551.3 | 678.5 | 805.7 | 933.0 |
| **20 rpm** | **φ (°)** | 29 | 484.4 | 596.2 | 708.0 | 819.8 | 1365.0 | 1680.0 | 1995.0 | 2310.0 | 289.7 | 356.6 | 423.4 | 490.3 |
| | | 30 | 512.8 | 631.2 | 749.5 | 867.9 | 1424.4 | 1753.1 | 2081.8 | 2410.5 | 300.0 | 369.2 | 438.5 | 507.7 |
| | | 36 | 722.6 | 889.4 | 1056.1 | 1222.9 | 1859.5 | 2288.7 | 2717.8 | 3146.9 | 447.9 | 551.3 | 654.7 | 758.0 |
| | | 38 | 811.0 | 998.1 | 1185.3 | 1372.4 | 2042.5 | 2513.8 | 2985.2 | 3456.5 | 573.6 | 706.0 | 838.4 | 970.8 |
| | | 41 | 966.2 | 1189.1 | 1412.1 | 1635.0 | 2364.9 | 2910.6 | 3456.3 | 4002.1 | 735.1 | 904.7 | 1074.3 | 1244.0 |

**Table 1. Installation power values for the parametric analysis for the models of Ghaly and Hanna (1991), Tsuha and Aoki (2010) and Sakr (2015) for D/d ratio of 2 in a cohesionless soil up to 10m depth, D=0.6m, d=0.3, p=1/3D and Blade thickness = 0.025m (from Spagnoli et al. in review).**

| Power at 10 m and with D=1,5(d) | | | Ghaly and Hanna | | | | Mohammed Sakr | | | | Cristina da Hollanda | | | |
|---|---|---|---|---|---|---|---|---|---|---|---|---|---|---|
| | | | γ (kN/m^3) | | | | γ (kN/m^3) | | | | γ (kN/m^3) | | | |
| | | | 13 | 16 | 19 | 22 | 13 | 16 | 19 | 22 | 13 | 16 | 19 | 22 |
| 5 rpm | φ (°) | 29 | 81.5 | 100.3 | 119.1 | 137.9 | 238.8 | 293.9 | 349.0 | 404.1 | 46.3 | 57.0 | 67.7 | 78.4 |
| | | 30 | 86.0 | 105.9 | 125.7 | 145.6 | 249.0 | 306.5 | 363.9 | 421.4 | 46.9 | 57.7 | 68.5 | 79.3 |
| | | 36 | 119.4 | 146.9 | 174.5 | 202.1 | 323.3 | 397.9 | 472.5 | 547.1 | 57.7 | 71.0 | 84.3 | 97.6 |
| | | 38 | 133.4 | 164.2 | 195.0 | 225.8 | 354.3 | 436.0 | 517.8 | 599.5 | 67.8 | 83.4 | 99.1 | 114.7 |
| | | 41 | 158.0 | 194.4 | 230.9 | 267.4 | 408.6 | 502.9 | 597.2 | 691.5 | 81.0 | 99.6 | 118.3 | 137.0 |
| 10 rpm | φ (°) | 29 | 163.0 | 200.6 | 238.2 | 275.8 | 477.6 | 587.8 | 698.1 | 808.3 | 92.6 | 114.0 | 135.4 | 156.8 |
| | | 30 | 172.1 | 211.8 | 251.5 | 291.2 | 498.0 | 612.9 | 727.8 | 842.8 | 93.7 | 115.3 | 137.0 | 158.6 |
| | | 36 | 238.8 | 293.9 | 349.0 | 404.1 | 646.5 | 795.7 | 944.9 | 1094.1 | 115.3 | 141.9 | 168.5 | 195.1 |
| | | 38 | 266.8 | 328.4 | 390.0 | 451.5 | 708.6 | 872.1 | 1035.6 | 1199.1 | 135.6 | 166.9 | 198.1 | 229.4 |
| | | 41 | 316.0 | 388.9 | 461.8 | 534.7 | 817.3 | 1005.9 | 1194.5 | 1383.1 | 161.9 | 199.3 | 236.6 | 274.0 |
| 15 rpm | φ (°) | 29 | 244.5 | 300.9 | 357.3 | 413.7 | 716.4 | 881.8 | 1047.1 | 1212.4 | 138.9 | 171.0 | 203.1 | 235.1 |
| | | 30 | 258.1 | 317.6 | 377.2 | 436.8 | 747.0 | 919.4 | 1091.8 | 1264.1 | 140.6 | 173.0 | 205.4 | 237.9 |
| | | 36 | 358.2 | 440.8 | 523.5 | 606.2 | 969.8 | 1193.6 | 1417.4 | 1641.2 | 173.0 | 212.9 | 252.8 | 292.7 |
| | | 38 | 400.2 | 492.6 | 585.0 | 677.3 | 1062.8 | 1308.1 | 1553.4 | 1798.6 | 203.4 | 250.3 | 297.2 | 344.1 |
| | | 41 | 473.9 | 583.3 | 692.7 | 802.1 | 1225.9 | 1508.8 | 1791.7 | 2074.6 | 242.9 | 298.9 | 355.0 | 411.0 |
| 20 rpm | φ (°) | 29 | 326.0 | 401.2 | 476.4 | 551.7 | 955.2 | 1175.7 | 1396.1 | 1616.6 | 185.3 | 228.0 | 270.8 | 313.5 |
| | | 30 | 344.1 | 423.5 | 502.9 | 582.4 | 996.0 | 1225.8 | 1455.7 | 1685.5 | 187.4 | 230.7 | 273.9 | 317.2 |
| | | 36 | 477.6 | 587.8 | 698.0 | 808.2 | 1293.0 | 1591.4 | 1889.8 | 2188.2 | 230.6 | 283.8 | 337.1 | 390.3 |
| | | 38 | 533.6 | 656.8 | 779.9 | 903.1 | 1417.1 | 1744.1 | 2071.2 | 2398.2 | 271.1 | 333.7 | 396.3 | 458.8 |
| | | 41 | 631.9 | 777.8 | 923.6 | 1069.4 | 1634.6 | 2011.8 | 2389.0 | 2766.2 | 323.8 | 398.6 | 473.3 | 548.0 |

**Table 2. Installation power values for the parametric analysis for the models of Ghaly and Hanna (1991), Tsuha and Aoki (2010) and Sakr (2015) for D/d ratio of 1.5 in a cohesionless soil up to 10m depth, D=0.45m, d=0.3, p=1/3D and Blade thickness = 0.025m (from Spagnoli et al. in review).**

Following the results of Tab. 1 and 2, the influence of the afore mentioned parameters, i.e. RPM, φ, γ and blade thickness has been assessed for a pile installed at 10m depth. Fig. 10A shows the influence of RPM on a sand with γ of 22 kN/m$^3$, φ of 41°, for a pile with D of 0.6m and d of 0.3 with a blade thickness of 0.025m. Notably, the model of Ghaly and Hanna delivers P values twice the model of Tsuha and Aoki. In turn, the model of Sakr give twice the values of P for the model of Ghaly and Hanna and it is four times higher than the value of Tsuha and Aoki

Fig. 10B shows the influence of the friction angle on the same pile properties. As for Fig. 10A, Ghaly and Hanna (1991) and Tsuha Aoki (2010) models follow the similar ratio with the Sakr (2015) model giving higher values, between 2 and 3.8 times the

values of the other two models. Fig. 10C shows the influence of γ on the power and for this parameter. In general, the response is very similar as observed previously. Fig. 10D shows the influence of the pitch on the P values. Considering that the response is also in this case similar in terms of model variability, increasing the pitch from 0.1m (i.e. 0.16D) to 0.6m (i.e. 1D), the power values considerably increasing, leading to P values as double as in comparison with the other three previous P values where geotechnical properties of the sands were modified.

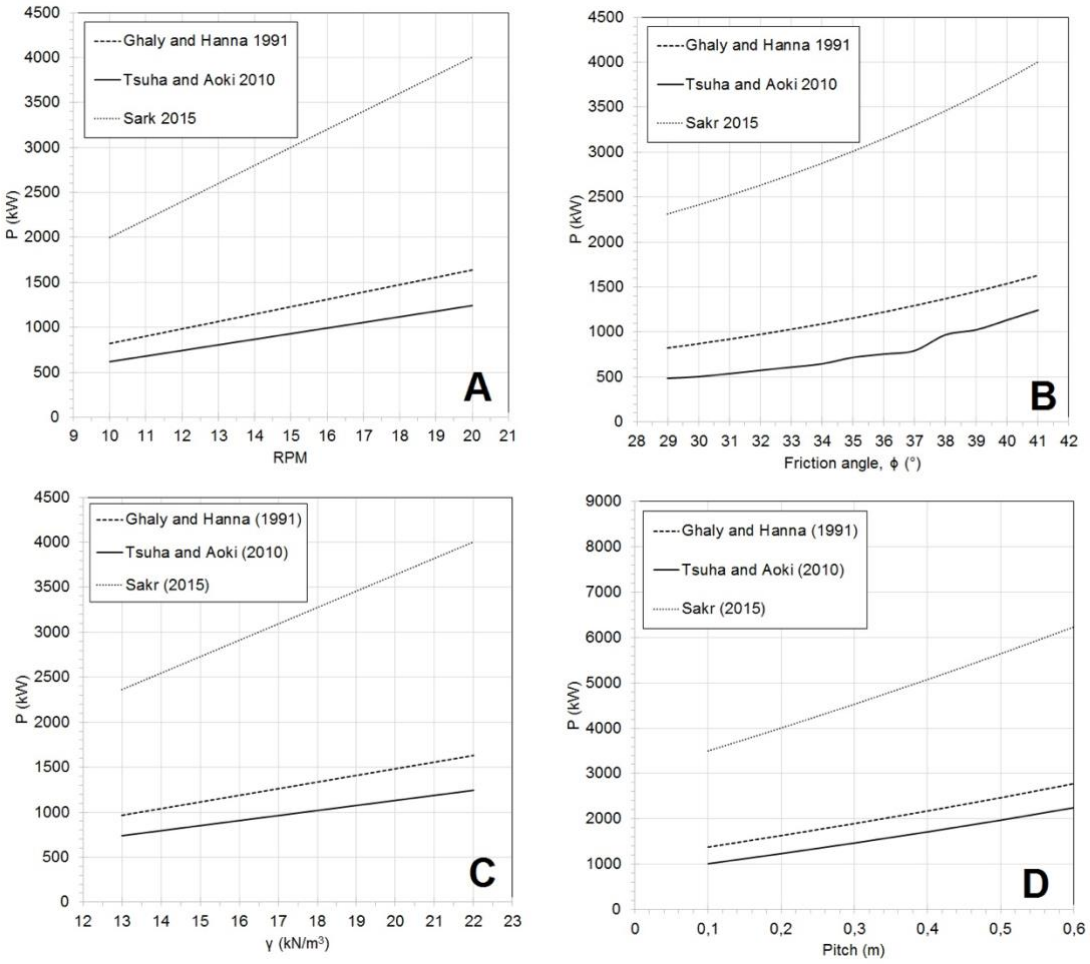


**Fig. 10 Influence of the RPM (A), friction angle (B), unit soil weight (C) and pitch (D) on the installation power for the three different models for a pile with D of 0.6m, d 0.3m and pitch of 1/3D (from Spagnoli et al. in review).**

Considering this behavior, by keeping constant the geotechnical properties of the sand and by changing the geometrical characteristics of the pile with respect to D and d, the power values dramatically change, reaching very high values. Fig. 11A shows a constant value of D arbitrary taken as 4m with a changing value of d in a sand assumed with a

friction angle of 41° and γ 22kN/m$^3$. By increasing the wing ratio, the model of Tsuaha and Aoki (2010) is barely influence by this; however, Ghaly and Hanna (1991) and Sakr (2015) models considerably decreases the P value for a wing ratio of 1.54 reaching 109MW for the Ghaly and Hanna model and 292MW for the Sakr model. The model of Tsuha and Aoki gives values for all over the D/d ratio from 44 to 46MW. For a constant D, the power estimated using Tsuha and Aoki model is not influenced by the variation of shaft diameter because, while the shaft diameter *d* is reduced, at the same time the helix surface increases. While during installation the torsional resistance mobilized along the shaft decreases, the torsional resistance mobilized at the helix surface increases in the same proportion; therefore, as the torque is the same for different d, the power should be also the same.

Simulating the same process but in a sand with smaller friction angle (i.e. 29°), the P value behavior is the same but the decreased by the half except for the model of Tsuha and Aoki which shows a decrease of about 20% (Fig. 11B).

Fig. 11C shows a constant d value arbitrary taken as 0.3m with changing D (and hence changing pitch) values. With respect with the Fig. 11A increasing the wing ratio (from 2 to 9) causes an increase in P values. P values are also considerably lower with respect to the values of Fig. 11A. Ghaly and Hanna shows P value as double as for the Tsuha and Aoki model, and in turn Sakr equation is 2.3 times higher than the model of Ghaly and Hanna. Fig. 11D shows the same model prediction but just as in case Fig. 11B with a sand with smaller friction angle (i.e. 29°). As for 8B, the power values decrease by the half if the sand has a smaller peak friction angle.

The different behavior of P with respect to the D/d ratio for Fig. 11A/B (constant D and variable d) and Fig. 11C/D (variable D and constant d) can be explained by the fact that all the three analyzed models calculate the torque using the relation D-d (with some variations with respect to the other). That is, when d is a constant value and D increases, torque also does it. If the opposite happens, i.e. D is constant and d increases, torque decreases. Such relations affect power in the same way.

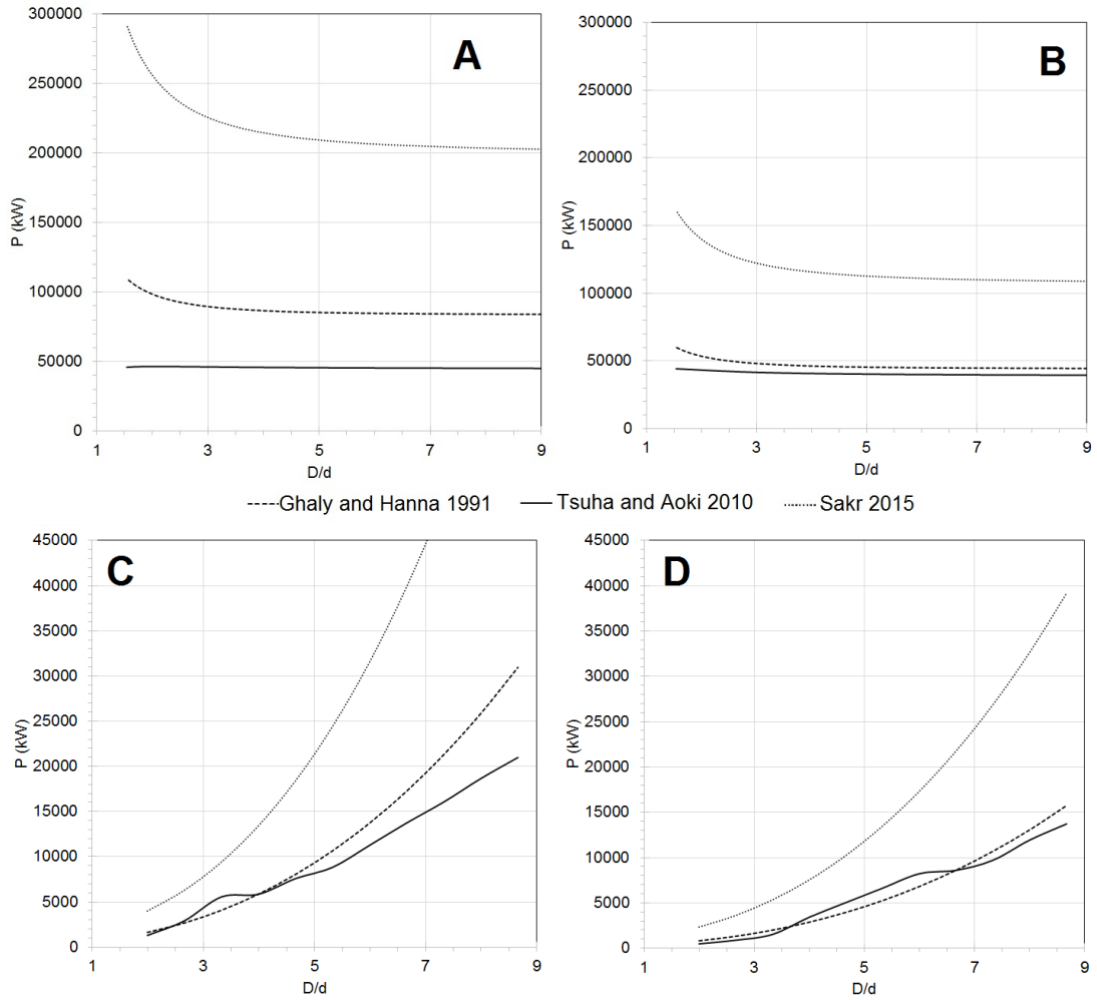


**Fig. 11 Constant value of D arbitrary taken as 4m with a changing value of d (A) with φ 41° γ 22kN/m$^3$ and a blade thickness of 0.025m; constant value of D arbitrary taken as 4m with a changing value of d (A) with φ 29° γ 22kN/m$^3$ and a blade thickness of 0.025m (B); constant value of d arbitrary taken as 0.3m with changing D and pitch (B) for a pile installed at 10m depth in a sand with φ 41°, γ 22kN/m$^3$ and a blade thickness of 0.025m (C) and constant value of d arbitrary taken as 0.3m with changing D and pitch (B) for a pile installed at 10m depth in a sand with φ 29°, γ 22kN/m$^3$ and a blade thickness of 0.025m (from Spagnoli et al. in review).**

# 4. PILE BEARING CAPACITY CALCULATIONS

## UPLIFT CAPACITY

Considering that the ultimate bearing capacity in compression is about 1.3 times higher than that of a screw pile in the pulling out tests (Trofimendkov and Mariupolskii, 1965), the maximum uplift capacity has been assumed as 0.75 of the axial compressive force as described earlier, considering therefore five different uplift loads namely 5, 10, 15, 20 and 25MN. Friction angle values of 30°, 35°, 40° and 45° have been considered to simulate typical values of the North Sea sand (Wu et al., 1987; Son, 2002), with a typical saturated unit weight of sand of 20kN/m$^3$ (e.g. Colombo and Colleselli, 1996).

Two different equations have been used to assess the maximum design depth for resisting the uplift loads evaluated in this paper. One is normally employed for "conventional" helical piles (CFEM 2006; Sakr, 2015). The uplift capacity is given by the sum of the bearing capacity above the helix and the skin friction pile/sand:

$$Q_u = Q_s + Q_h \tag{32}$$

Where $Q_s$ is the fraction related to shaft resistance and $Q_h$ is the fraction related to the helix uplift resistance. The shaft resistance is given as (CFEM, 2006):

$$Q_s = \pi \cdot d \cdot L \cdot q_s \tag{33}$$

Where $d$ is shaft diameter, $L$ is the length in which shaft friction is considered and $q_s$ is the average unit shaft friction of soil, given as

$$q_s = \sigma'_v K_s \tan(\delta_{cv}) \tag{34}$$

Where $\sigma'_v$ is the effective vertical pressure at the mid depth of the pile, $K_s$ is the coefficient of lateral earth pressure assumed as $K_s = 2(1 - sin\phi)$ for torque driven piles (Sakr, 2015) and $\delta_{cv}$ is the constant volume interface friction angle. In the current work, the value of $\delta_{cv}$ has been assumed as 29° considering a fine-sand granulometry (Lehane et al., 2005). According to Jardine et al. (1993) $\delta_{cv}$ seems to be the most appropriate frictional parameter for piles in sand and does not depend on the relative density of the soil, but varies with the sand mean grain size $D_{50}$.

The ultimate uplift capacity $Q_h$ of the helix can be estimated from the following expression:

$$Q_h = A_h \cdot \gamma \cdot z \cdot F_q \quad (35)$$

Where $A_h$ is the projected helix area, $\gamma$ is the average unit weight of the soil, $z$ is the depth of a helix and $F_q$ is the breakout factor of a helix.

In the current work, as deep-anchors were considered the breakout factor becomes constant after a critical embedment depth (for greater embedment depths, a local shear failure in soil located around the anchor takes place). For embedment depths greater than $10D$, we used the values of $F_q$ proposed in the A.B. Chance Co. (2010). They recommend lower values of $F_q$ to reproduce the performance of helical anchors influenced by the soil disturbance caused by pile installation.

The other equation is very popular in Japan for assessing the uplift capacity of large helical piles (Japan Road Association, 2007):

$$Q_u = \pi \cdot D \cdot \left(\gamma \cdot L + \gamma \cdot \frac{H}{2}\right) \cdot H \cdot \beta \cdot tan\phi + U \cdot L \cdot q_s \quad (36)$$

Where $Q_U$ is the ultimate pull-out resistance of pile determined from ground base, $D$ the helix diameter, $\gamma$ unit weight of the layer from surface above bearing layer $L$ is the length in which shaft friction is considered, $H$ is length of the shear failure zone above helix and defined by the Japan Road Association (2007) as ≤2.5D, $\beta$ is the pull-out factor which corresponds to the Meyerhof's coefficient for foundation uplift (lateral earth pressure coefficient in uplft, $K_u$), $\phi$ is the internal friction angle of bearing layer, $U$ is the perimeter of pile and $q_s$ is the skin friction (see equation 3).

As discussed by Nagata and Hirata (2005), the earth pressure acting in the shear cylinder just above the helix formed a trapezoidal curve: it increased to nearly equal to $K_p$ near the wing, and it decreased to a value nearly equal to the earth pressure at rest, $K_0$ , at about 2D above the helix. Based on this previous observation, in the current paper we took $H = 2D$ as also employed by Japanese companies (e.g. Mori, 2003).

After having assessed the maximum depth to resist the uplift capacity values, the torque equation of Tsuha and Aoki (2010) has been employed to assess the maximum torque to reach the design depth.

## INSTALLATION TORQUE

Tsuha and Aoki (2010) presented a relationship between uplift capacity and installation torque for deep helical piles in sand. Centrifuge and direct shear interface tests, were carried out with dry Fontainebleau sand samples to evaluate the proposed theoretical relationship. The equation stablished in this model are the following:

$$T = \frac{Q_s d}{2} + \frac{\sum_{i=1}^{N} Q_h d_c \tan(\theta + \delta_{cv})}{2} \quad (37)$$

Where $Q_s$ is shaft resistance, $d$ is diameter of the anchor's shaft, $Q_h$ is ultimate uplift capacity of a helix, $d_c$ is diameter of a circle corresponding to the helix surface, $\theta$ is helix angle and $\delta_{cv}$ is constant volume interface friction angle. Equation 6 shows that the installation torque can be estimated simply from the results of uplift capacity of helical piles (uplift capacity $Q_h$ of the helix and the shaft resistance $Q_s$). As in this work two different equations are used to calculate the uplift capacity of helical piles, for each case of pile two values of estimated installation torque are presented.

## INDUCED SHEAR STRESS ACTING IN THE PILE

Considering the installation depths and in turn the torque values, the yield strength of the pile has also been assessed, which depends on the steel type, wall thickness and installation torque assessment. Torque calculation is, in fact, needed also to assess the yield strength of the pile, in order not to damage it (Spagnoli and Gavin, 2015). Looking at Fig. 12, the induced shear stress within the ring, $\tau$, is defined as:

$$\tau = a \cdot r \quad (38)$$

Where $a$ is the angular coefficient of the straight line and $r$ is distance from the section center. Considering a small section of the ring we observe the following:

$$[\tau \cdot dA] \cdot r = dT \quad (39)$$

Which can be further developed as:

$$[(a \cdot r) \cdot (r \cdot dr \cdot d\theta)] \cdot r = dT \quad (40)$$

Where $d\theta$ is the infinitesimal angle in the polar coordinates. The unknown value in the previous equations (38 to 40) is the angular coefficient, $a$. To get its value, the ring surface has to be integrated:

$$T = \int_0^{2\pi} \int_{r_{int}}^{r_{ext}} a \cdot r^2 \cdot dr \cdot d\theta \cdot \mathrm{r} = a \int_0^{2\pi} \int_{r_{int}}^{r_{ext}} r^3 \cdot dr \cdot d\theta \quad (41)$$

Where the $r_{ext}$ is the external radius and $r_{int}$ internal radius of the pile.

Which gives:

$$T = 2 \cdot \pi \cdot a \left[\frac{r_{ext}^4}{4} - \frac{r_{int}^4}{4}\right] \quad (42)$$

Solving the integration, we obtain $a$:

$$a = \frac{2 \cdot T}{\pi \cdot (r_{ext}^4 - r_{int}^4)} \quad (43)$$

The induced shear stresses the pile can resist is given by:

$$\tau_{max} = a \cdot r_{ext} \quad (44)$$

Substituting the value of the angular coefficient in equation 43 we obtain:

$$\tau_{max} = \frac{2 \cdot T \cdot r_{ext}}{\pi \cdot (r_{ext}^4 - r_{int}^4)} \quad (45)$$

To verify the yield strength of steel we need to use the Tresca's criterion:

$$\sigma_{id,max} = \sqrt[2]{\left(\frac{V}{A}\right)^2 + 3 \cdot {\tau_{max}}^2} \quad (46)$$

Where $\sigma_{id,max}$ is the maximum ideal stress on the external ring of the pile at the surface (where the stress condition is critical), which has to be compared with the yield strength of the pile, V is vertical force; A is the circumferential area of the pile which is $A = \pi(r_{ext}^2 - r_{int}^2)$, considering d value of 500mm and a wall thickness of 12.5mm estimated by the relation suggested by Randolph et al. (2005) where the shaft diameter is related to the wall thickness of a factor of about 40.

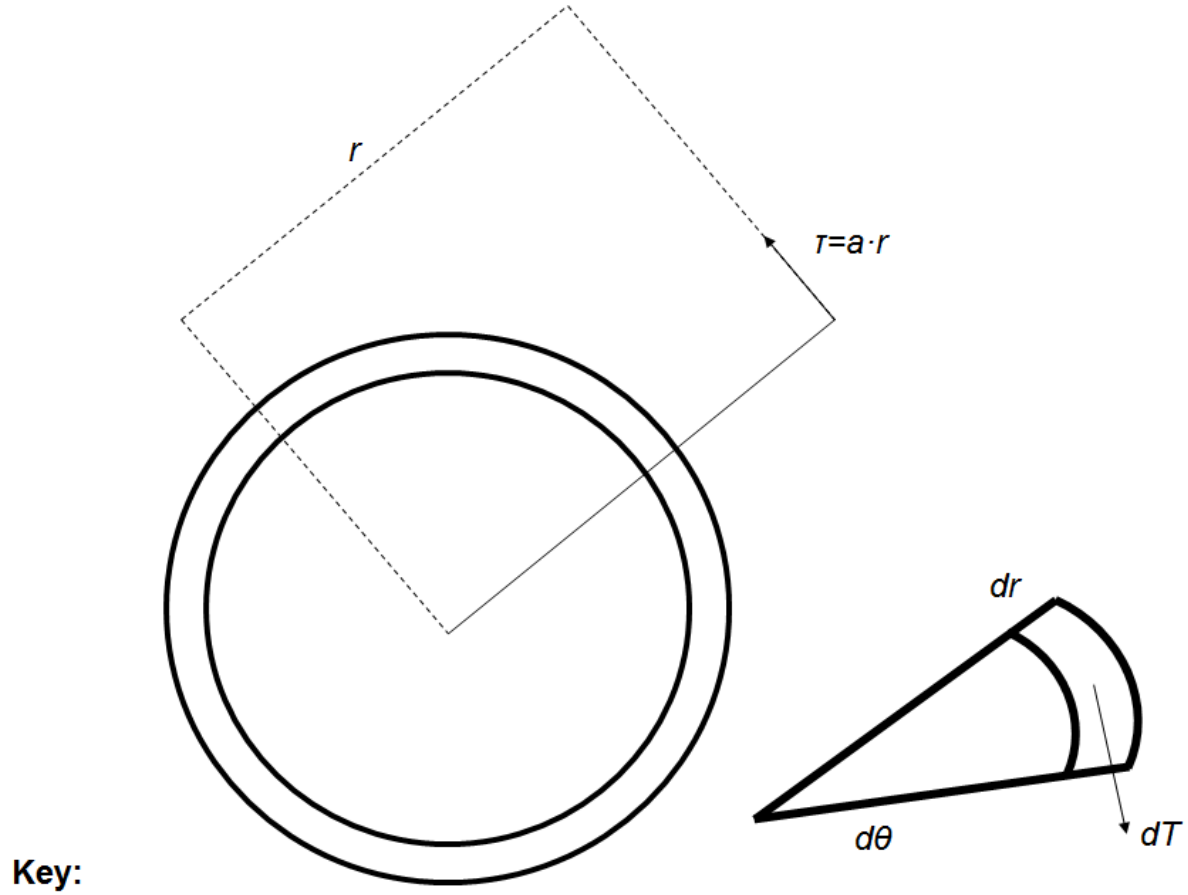


**Key:**

| | |
|---|---|
| *a* | angular coefficient |
| *r* | distance from the section center |
| *dr* | infinitesimal distance from the section center |
| *dT* | infinitesimal torque |
| *dθ* | infinitesimal angle in the polar coordinates |
| *τ* | induced shear stress within the pile |

**Fig. 12 Relation regarding the torque and the yield resistance of the pile (from Spagnoli et al. in review)**

## INSTALLATION POWER CALCULATION

In addition, the calculation of the power (P) required to install helical foundations is fundamental for the selection of the most appropriate equipment to guarantee a successful installation. Therefore, the P value is used instead of torque. P is the energy developed in the unit of time. P is an interesting parameter because it permits to know the specifications required of the machine to install a pile in a soil with different geotechnical properties. The values of power are given by following equation:

$$P = P(T) + P\,(V) = T\omega + V\frac{\omega}{2\pi}p \qquad (47)$$

$$v = \frac{\omega}{2\pi} p \tag{48}$$

The power related to the vertical force, $P\ (V)$, is calculated considering the downward vertical force ($V$) following the equations of Ghaly and Hanna (1991), as no other equations have been found to get this parameter. However, as Sakr (2015) stated, "*crowd force is typically not measured during installation even though additional crowd forces are generated during pile installation as a result of engaging helices into soil and as pile advancing into ground*".

The results show an abacus relating the given embedment depth for a given uplift force with the installation torque and power needed to reach the design depth.

# 5. PROPOSAL OF DESIGN TECHNIQUES FOR THE SCREW PILES, IN RELATION TO THE TORSIONAL MOMENT DEVELOPING DURING THE INSTALLATION AND UPLIFT CAPACITY.

Because mainly helical piles are used for relative low capacity loads (about 600kN), the installation torque (and power) is also limited (e.g. Bobbit and Clemence, 1987). However, using the correlation uplift capacity-torque (Tsuha and Aoki, 2010), for offshore application high torque values are expected.

For the determination of the pile depth required to resist uplift forces of 5, 10, 15, 20 and 25 MN, several calculations have been performed considering the conventional uplift capacity method (equations 33 and 35) and the Japanese code (equation 36). The calculation has been assumed in an effective stress state of the sand. Following the estimation of the depth, the installation torque by means of the Tsuha and Aoki model (2010) has been assessed. To design the installation rotary, the installation power has been also estimated by using equation 16 for different RPM values and graphically shown.

Fig. 13 shows an abacus in order to obtain the design depth and the corresponding installation torque for three piles: A is a pile with D of 750mm and d of 500 (wing ratio 1.5), B is a pile with D of 1000mm and d of 500 (wing ratio 2) and C is a pile with D of 1250mm and d of 500 (wing ratio 2.5). The pitch, $p$, is taken as 1/3 of D as normally employed by Japanese contractors (e.g. Tadashi and Mikio, 2009). The blade thickness has been constantly assumed as 25mm.

Each graph contains the calculated uplift capacity according to the "conventional" uplift bearing capacity equation, i.e. equations 33 and 35 (left hand-side of the figure) and the Japanese code, i.e. equation 36 (right hand-side of the figure) considering the typical axial loads acting on the pile (see above in the paper).

In order to obtain the predicted depth and the corresponding torque, a graphical example is shown in Fig. 13 (upper figure on the left side). Knowing the friction angle of the sand, a line (in blue) is drawn upward to meet the uplift force symbol (circle) and the corresponding torque (square). Each uplift capacity values from 5 to 25MN is shown in the graph. When the desired uplift capacity value is met (indicated by the corresponding

line), if the line is drawn to the left the design depth is obtained; if the line corresponding to the torque is met, the blue line is drawn to the right to obtaining the predicted torque.

For the case shown in Fig. 13 (conventional uplift equation) assuming a friction angle value for the sand of 40°, if the pile has to resist an uplift force of 5MN, the pile with D 750mm and d 500mm has to be installed at a depth of 25m with a torque of 1.2MNm.

To compare the results with the values obtained by the Japanese code, on the right-hand side of the figure 13, we draw a red line from the friction angle of 40°, meeting the desired uplift capacity and the corresponding torque value. The Japanese equation give a design depth of 23.4m and a torque of 1MN, which is slight less if compared with the results obtained with the conventional equation.

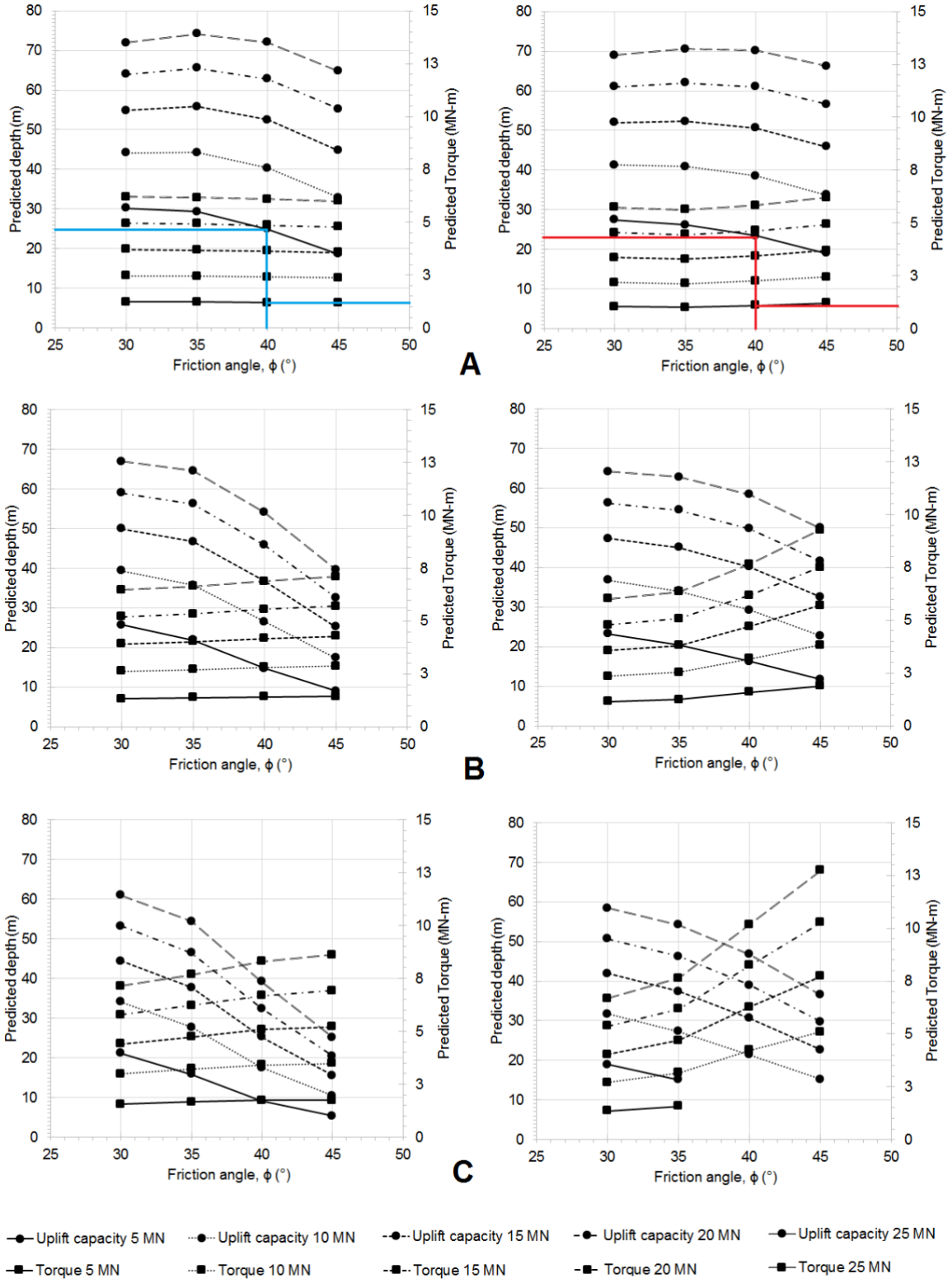


**Fig. 13 Graphical abacus for the estimation of the design depth and torque for a pile with D 750mm and d 500mm (A), D 1000mm and d 500mm (B) and D 1250mm and d 500m (C). The left diagrams refer to the conventional bearing capacity equation, the right diagrams refer to the Japanese code (from Spagnoli et al. in review).**

Tab. 3 to 5 summarizes the values shown in Fig. 13. For the sake of clarity as the Japanese equation are valid for deep piles, depth with values less than 10D were not considered in the Fig. 13. It is interesting to note that the conventional uplift equation give design depth values about 10% higher with respect to the Japanese equation. However, for increasing friction angle values, the depths obtained by the Japanese equation become slightly higher (about 2%). For the largest piles (D=1250mm), and for increasing friction angle values the depths calculated by the Japanese equation are about 20% higher than for those obtained with the conventional equations.

As per the design depth, consequently the torque values are (for the depth obtained by the conventional equation) slightly higher than for the depth obtained by the Japanese equation. As only the model of Tsuha and Aoki (2010) was used to assess the torque capacity, the difference is given by the design depth. For depth values obtained with the conventional equations, torque is about 20% higher with respect to the values obtained with Japanese code. However, for increasing friction angle values and pile helix diameter, the torque obtained for the Japanese code becomes up to 30%. Besides, it is noted that the torque obtained for the conventional depth calculation for the smaller pile barely changes or it is slightly low (only one place after the decimal point).

The differences mentioned above occur because the model proposed in Tsuha and Aoki (2010) to estimate the final installation torque of helical foundations assumes that the final installation torque is proportional to the uplift capacity. Therefore, as for the estimated values of the helix uplift capacity ($Q_h$), using the Japanese equation, the length of pile needed to support a certain load obtained is lower, and consequently the installation torque should be also lower. This tendency is inverse for higher friction angle values.

As shown in Table 3 to 5 and Fig. 14, the differences of the final installation depth considering that the Japanese code equation is recommended for helical piles with a minimum length of 10D and final torque seems to be more important for the pile cases of greater helix diameter.

| Qu (MN) | φ (°) | Conventional equation | | Japanese equation | |
|---|---|---|---|---|---|
| | | H (m) | Torque (MN-m) | H (m) | Torque (MN-m) |
| 5 | 30 | 30.2 | 1.2 | 27.4 | 1.04 |
| | 35 | 29.4 | 1.2 | 26.2 | 1.01 |
| | 40 | 25.0 | 1.2 | 23.4 | 1.09 |
| | 45 | 18.6 | 1.2 | 19.0 | 1.20 |
| 10 | 30 | 44.1 | 2.5 | 41.3 | 2.18 |
| | 35 | 44.3 | 2.5 | 40.9 | 2.13 |
| | 40 | 40.3 | 2.4 | 38.6 | 2.25 |
| | 45 | 32.8 | 2.4 | 33.7 | 2.45 |
| 15 | 30 | 54.9 | 3.7 | 52.0 | 3.36 |
| | 35 | 55.8 | 3.7 | 52.3 | 3.28 |
| | 40 | 52.5 | 3.6 | 50.7 | 3.44 |
| | 45 | 44.8 | 3.6 | 45.9 | 3.69 |
| 20 | 30 | 63.9 | 5.0 | 61.0 | 4.53 |
| | 35 | 65.6 | 4.9 | 62.0 | 4.45 |
| | 40 | 62.9 | 4.9 | 61.0 | 4.63 |
| | 45 | 55.3 | 4.8 | 56.6 | 4.94 |
| 25 | 30 | 71.9 | 6.2 | 69.0 | 5.73 |
| | 35 | 74.2 | 6.2 | 70.6 | 5.63 |
| | 40 | 72.1 | 6.1 | 70.2 | 5.83 |
| | 45 | 64.8 | 6.0 | 66.3 | 6.19 |

**Tab. 3 Results obtained by the calculations using the conventional and Japanese equations for five different uplift forces, 4 friction angles and 3 different piles. D=0.75m and d=0.5m (from Spagnoli et al. in review).**

| Qu (MN) | φ (°) | Conventional equation | | Japanese equation | |
|---|---|---|---|---|---|
| | | H (m) | Torque (MN-m) | H (m) | Torque (MN-m) |
| 5 | 30 | 25.7 | 1.3 | 23.3 | 1.1 |
| | 35 | 21.9 | 1.4 | 20.3 | 1.3 |
| | 40 | 14.7 | 1.4 | 16.2 | 1.6 |
| | 45 | 9.0 | 1.4 | 11.7 | 1.9 |
| 10 | 30 | 39.4 | 2.6 | 36.8 | 2.4 |
| | 35 | 35.7 | 2.7 | 34.1 | 2.5 |
| | 40 | 26.5 | 2.8 | 29.3 | 3.2 |
| | 45 | 17.4 | 2.9 | 22.7 | 3.8 |
| 15 | 30 | 50.0 | 3.9 | 47.3 | 3.6 |
| | 35 | 46.8 | 4.0 | 45.0 | 3.8 |
| | 40 | 36.7 | 4.2 | 40.2 | 4.7 |
| | 45 | 25.2 | 4.3 | 32.6 | 5.7 |
| 20 | 30 | 59.0 | 5.2 | 56.2 | 4.8 |
| | 35 | 56.2 | 5.3 | 54.4 | 5.1 |
| | 40 | 45.8 | 5.6 | 49.7 | 6.2 |
| | 45 | 32.6 | 5.7 | 41.6 | 7.5 |
| 25 | 30 | 66.9 | 6.5 | 64.1 | 6.0 |
| | 35 | 64.6 | 6.6 | 62.8 | 6.3 |
| | 40 | 54.0 | 6.9 | 58.4 | 7.7 |
| | 45 | 39.6 | 7.1 | 49.9 | 9.3 |

**Tab. 4 Results obtained by the calculations using the conventional and Japanese equations for five different uplift forces, 4 friction angles and 3 different piles. D=1m and d=0.5m (from Spagnoli et al. in review).**

| Qu (MN) | φ (°) | Conventional equation | | Japanese equation | |
|---|---|---|---|---|---|
| | | H (m) | Torque (MN-m) | H (m) | Torque (MN-m) |
| 5 | 30 | 21.1 | 1.6 | 19.0 | 1.4 |
| | 35 | 15.8 | 1.7 | 15.1 | 1.6 |
| | 40 | 9.2 | 1.7 | 11.0 | 2.1 |
| | 45 | 5.3 | 1.7 | 7.3 | 2.4 |
| 10 | 30 | 34.1 | 3.0 | 31.7 | 2.7 |
| | 35 | 27.7 | 3.2 | 27.3 | 3.2 |
| | 40 | 17.5 | 3.4 | 21.4 | 4.2 |
| | 45 | 10.5 | 3.5 | 15.2 | 5.1 |
| 15 | 30 | 44.4 | 4.4 | 41.9 | 4.0 |
| | 35 | 37.7 | 4.7 | 37.4 | 4.7 |
| | 40 | 25.3 | 5.1 | 30.6 | 6.3 |
| | 45 | 15.5 | 5.2 | 22.7 | 7.7 |
| 20 | 30 | 53.2 | 5.8 | 50.7 | 5.4 |
| | 35 | 46.5 | 6.2 | 46.3 | 6.2 |
| | 40 | 32.4 | 6.7 | 39.0 | 8.2 |
| | 45 | 20.4 | 6.9 | 29.8 | 10.3 |
| 25 | 30 | 61.0 | 7.1 | 58.4 | 6.7 |
| | 35 | 54.4 | 7.7 | 54.2 | 7.6 |
| | 40 | 39.2 | 8.3 | 46.8 | 10.2 |
| | 45 | 25.2 | 8.6 | 36.5 | 12.8 |

**Tab. 5 Results obtained by the calculations using the conventional and Japanese equations for five different uplift forces, 4 friction angles and 3 different piles. D=1.25m and d=0.5m (from Spagnoli et al. in review).**

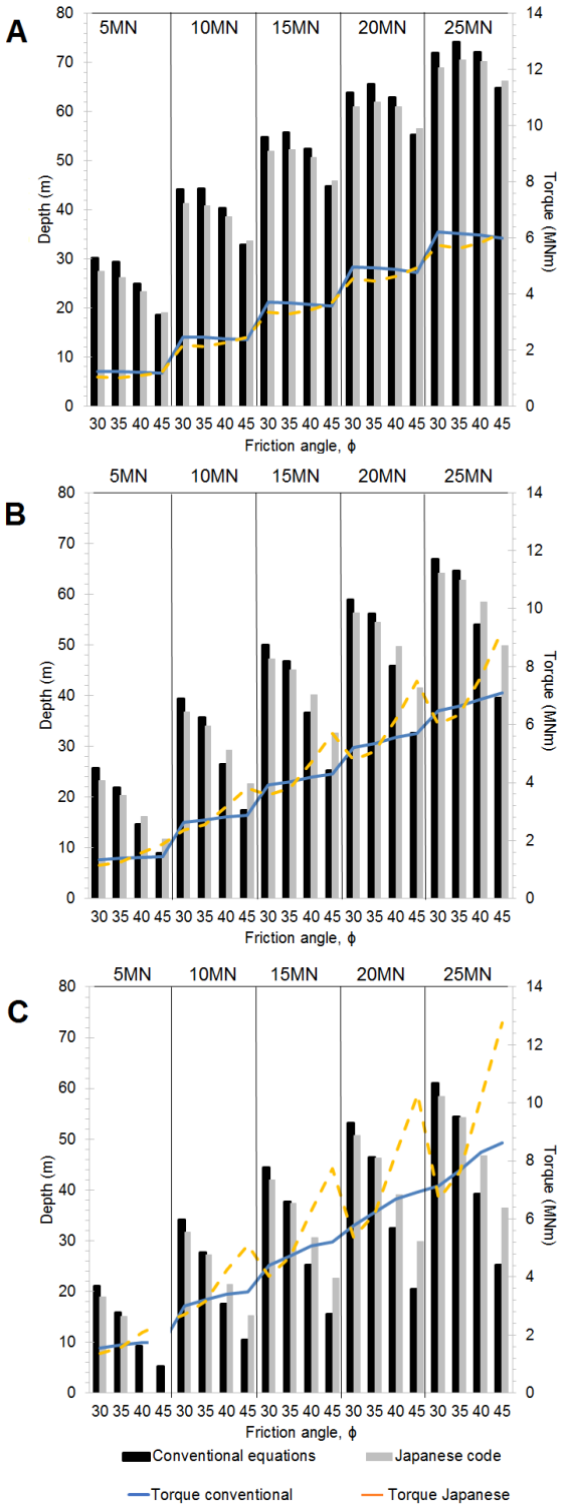


**Fig. 14 Diagram showing the relation installation depth to installing torque for different friction angle soils for the small pile (D 750mm) (A), medium pile (D 1000mm) (B) and large pile (D1250mm) (C). For the largest pile depth and torque for 5MN uplift load for 40° and 45° friction angle values are not shown (see Tab. 3 to 5 for detail) (from Spagnoli et al. in review).**

Considering Fig. 13 and Tab. 3 to 5 a visual summarize of the results is shown in Fig. 14. From Fig. 14 it is possible to state:

1. Torque increases with the increasing helix diameter D for the same geotechnical properties of the sand, here represented by the soil friction angle;
2. Due to the different equations used to estimate the helix uplift capacity $Q_h$ torque also changes (the equation to estimate the installation torque is based on pile capacity). The changes in torque values are larger for the largest pile (D=1250mm);
3. Japanese equation give estimated pile depth values smaller than for that obtained for the conventional equation;
4. For the largest pile and uplift force of 5MN, depth values according to the Japanese equation for friction angle of 40° and 45° were lower than 10D therefore they were not considered in the discussion. Corresponding torque was also not considered;
5. For higher uplift capacity values the differences regarding the estimated depth become larger for all three piles considered in this research;
6. For higher uplift capacity values and higher friction angle values the Japanese equation estimates larger depth than the conventional equation.

For this study a constant volume interface friction angle, $\delta_{cv}$, of 29° has been assumed following the ICP-05 guidelines modified by Lehane et al. (2005) for fine sand with the mean effective particle size $D_{50}$ (lower than 0.2mm). These authors showed that the $\delta_{cv}$ values increase as the roughness normalized by the $D_{50}$ increases. As consequence, for a particular pile roughness the interface friction angle between the sand and pile decreases as $D_{50}$ increases.

In order to investigate the influence of the grain size on the uplift capacity and in turn on torque, two other $\delta_{cv}$ values, i.e. 23° and 26° ($D_{50}$ values of 0.35 and 2 mm respectively) of according to the trend recommended by the ICP-05 guidelines, has been investigated for the medium pile (i.e. D=1000mm) for the uplift capacity of 15MN. Results are shown in Fig. 15. It is possible to note that the variation in terms of depth assessments are not large among each method (up to 5% difference for depth) and also the torque values is similar for all three different $\delta_{cv}$, considering however that the torque slightly increases with increasing $\delta_{cv}$ values. Notably, there is a reverse behavior

in terms of depth, as observed previously: for larger friction angle values (40° and 45°) the depth obtained with the Japanese equation are larger than the depth values for the conventional equation.

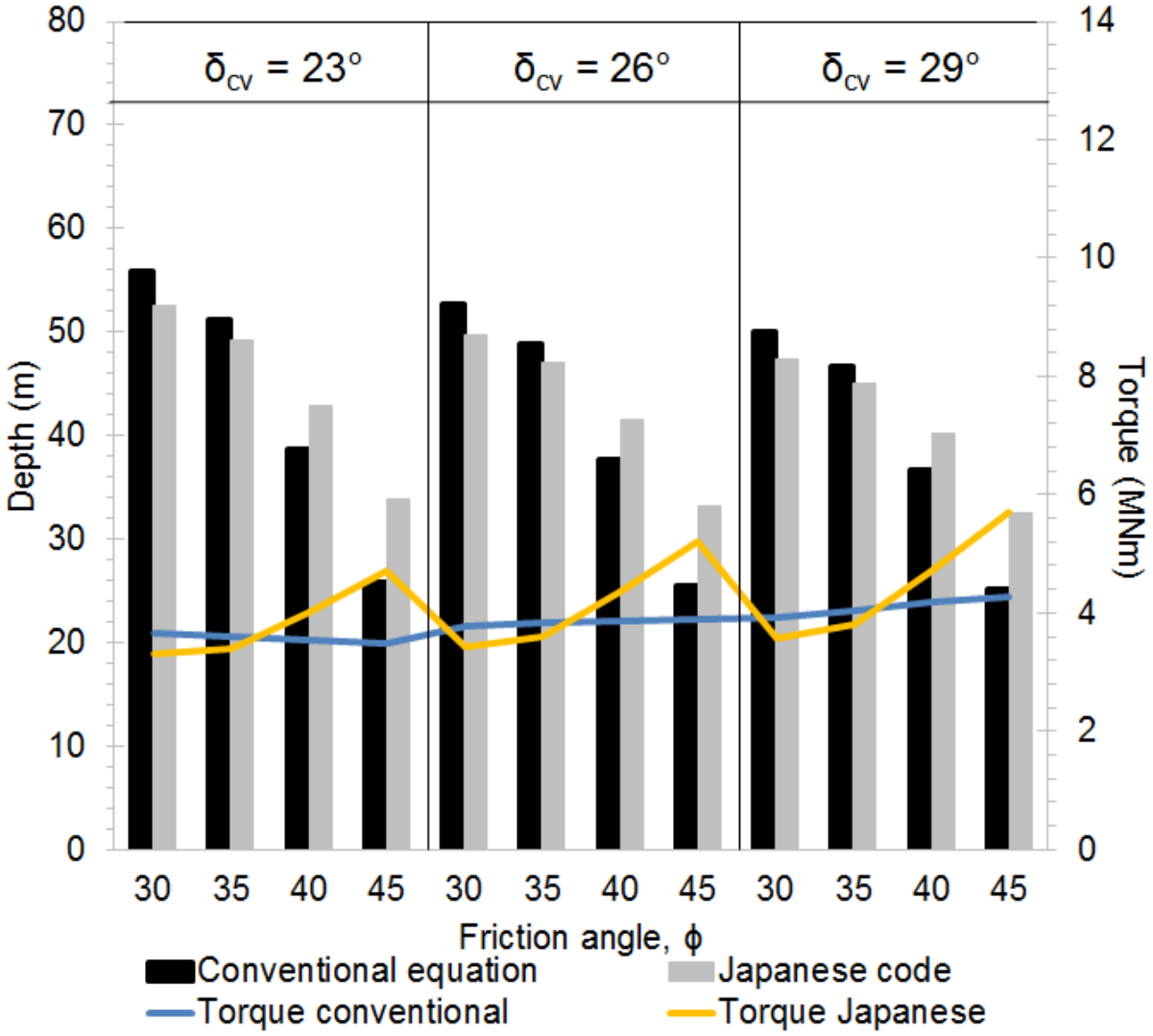


**Fig. 14 Influence of the constant volume interface friction angle, $\delta_{cv}$, on the installation depth and the resulting installation torque as an example on the medium pile (D=1000mm) for an uplift force of 15MN (from Spagnoli et al. in review).**

In order to properly design the rotary head for the pile installation the torque alone is necessary but not sufficient.

Fig. 16 shows three diagrams where starting from the obtained torque, the necessary power is obtained which depends on the RPM values.

Considering the example before, and assuming a 1.2MNm torque for installing a pile with D of 750mm and d 500mm in a sand with 40° ϕ for resisting 5MN uplift force is needed, the power of the motor will be 3.37MW if 20 RPM are employed.

If we, instead, use the installation torque results coming from the $Q_h$ values obtained using Japanese code, considering an installation torque of 1MN in order to install the same pile in the same sand with 20 RPM a motor giving 3.04MW is necessary, which is 10% less powerful than the one used if the conventional equations are used. As mentioned previously in this paper, the estimated length of pile needed to support a certain uplift load using has an influence on the installation torque and power.

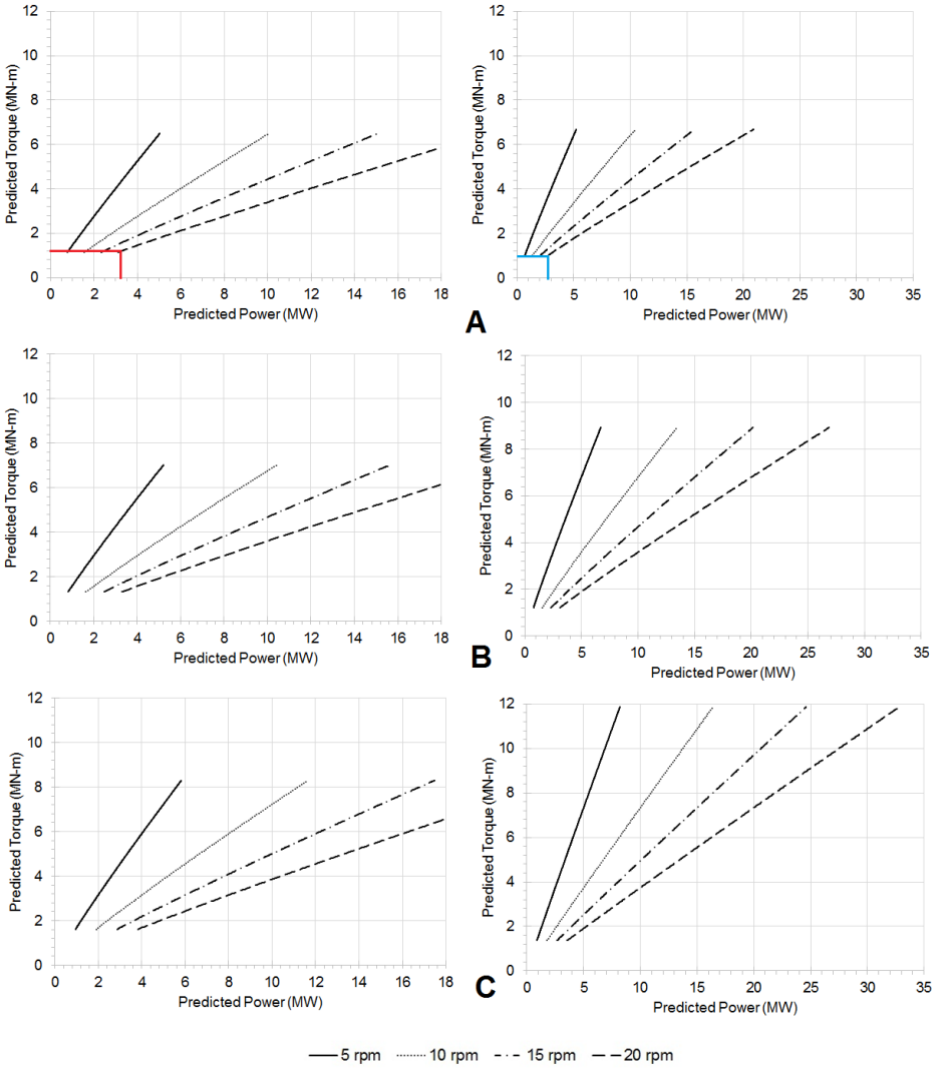


**Fig. 16 Estimation of the installation power for a pile with D 750mm and d 500mm (A), D 1000mm and d 500mm (B) and D 1250mm and d 500m (C) with the conventional equation (left side) and Japanese equation (right side) (from Spagnoli et al. in review).**

Consequently, the power values obtained for the torque needed to install a pile considering the Japanese code tend to be lower than the results obtained with the conventional equation but the trend reverses with increasing friction angle values. This trend is the same for the different RPM values.

Another verification which has been made is regarding the yield strength of the pipe steel. As a reference value for the steel, the A36 steel has been considered. Its yield strength is of 250MPa, with an ultimate tensile strength of 400-550 MPa and a density of 7.8 g/cm$^3$ (Steel Construction Manual, 1986). Considering the values obtained for this research, from the 120 examples investigated obtained only one showed maximum ideal stress in the pile lower than 250MPa, which is the largest pile installed in a sand with $\phi$ 45° for an uplift value of 5MN.

This is an important aspect to consider when helical piles are taken into account as offshore pile systems. It seems in fact that one pile system with these characteristics is not able to withstand the strong torque values required to reach the depth for the given axial tensile force. The best option would be to increase the number of piles per foundation leg. However, from the practical point of views, this means that several installation torque machines should work in a limited space for installing two or more piles simultaneously.

# CONCLUSIONS

The models of Sakr (2015) and Ghaly & Hanna (1991) are theoretical equations proposed to be used to estimate the installation torque of helical piles in sand for field (in situ) conditions but the models of Ghaly and Hanna did not include in their equations the effective stresses due to the evaluation of their model test in dry sand, while Sakr proposed the use of effective stresses, for helical piles in saturated sand his model is more appropriated. Nonetheless, evaluating the model of the equations proposed by comparing them with measured results, Ghaly and Hanna used the results of reduced scale model tests and Sakr used results of field tests.

In the case of Tsuha and Aoki (2010) model, the installation torque is a function of the uplift capacity. Therefore, as the uplift capacity varies with the effective stresses, this model can be used for dry and for saturated sand.

To estimate the breakout factor Nq value for helical anchors in sand for the models used, it is recommendable the chart of Vesic (1971) appropriated to helical anchors. So, to simulate the variation of torque along the depth, we should use Nq varying with the embedment depth of the helix (H/D) for depths lower than 8D (8 times the helix diameter), after this critical depth the Nq values are constant. However, to use the chart of Vesic (1971) to find Nq, it used friction angle in critical state $\delta_{cv}$ assumed as 29°. It is necessary a smaller le $\delta_{cv}$ because the installation effect of the soil penetrated by the helix modify the sand initial condition.

A parametric analysis considering 520 calculations have been performed considering the well-known torque models of Ghaly and Hanna (1991), Tsuha and Aoki (2010) and Sakr (2015) in dry cohesionless soils. The models have been first assessed against lab installation piles in a dense sand. The results show that among the three models, the equations of Tsuha and Aoki (2010) showed better agreement, above all for the last part of installation, whereas the model of Sakr gave higher estimated torque values.

The parametric analysis showed that the power increases for denser sand (higher friction angle and unit weight values), higher round per minute (RPM) installation values. High pitch values (by keeping constant the other geometrical properties of the pile) also considerably increases the power values.

By performing a calculation in a loose sand (φ 29°) and dense sand (φ 41°,) with a fixed value of γ (22kN/m$^3$) and a blade thickness (0.025m), and changing the wing ratio first by keeping constant D and varying d and then by keeping constant d and varying D, extremely high power values were obtained. It was observed that the power decreases for the former (D constant, d changing) and increases for the latter (D changing, d constant). This behavior can be explained by the fact that all the three analyzed models calculate the torque using the general relation D-d. That is, when d is a constant value and D increases, torque also does it. If the opposite happens, i.e. D is constant and d increases, torque decreases.

In the thesis is also analyzed two different uplift capacity equations (a conventional one and another from the Japanese code) for helical piles in the light of a possible offshore application of these piles in cohesionless soils. After having selected four friction angle values and assumed 5 uplift loads (from 5 to 25MN), by considering a constant interface friction angle pile/soil $\delta_{cv}$ of 29°, results show that torque values (calculated with the equation of Tsuha and Aoki, 2010) increase with increasing helix diameter D for the same geotechnical properties of the sand (i.e. soil friction angle in this work). Besides, the Japanese equation give estimated embedment pile depth values larger than for that obtained for the conventional equation. Installation power has also been assessed considering the RPM and torque values for a possible rotary drive needed for installing these structures. An important point was observed: assuming yield strength of a steel of 250MPa, the torque values obtained result too high for the yield strength of the pile for all 120 cases analyzed, except one. This means that likely more piles for each leg are required. Although from the design point of view this is the best option, from the construction point of view, it will be difficult to arrange casing machine oscillators installing simultaneously two or more pile at each leg from an installation barge.

# BIBLIOGRAPHY

A.B. Chance 2010. Guide to Model Specification CHANCE® Civil Construction: Helical Piles for Structural Support. Bulletin 01-0303. Shelton, CT: Hubbell Inc.

Al-Baghdadi, T.A., Brown, M.J., Knappett, J.A., and Ishikura, R. 2015. Modelling of laterally loaded screw piles with large helical plates in sand. In Frontiers in Offshore Geotechnics III. Edited by V. Meyer. Taylor & Francis Group, London, pp. 503-508.

Aydin, M., Bradka, T., Kort, D., 2011, Osterberg cell load testing on helical piles. Geo-Frontiers 2011, pp. 66–74.

Arup Geotechnics 2005. Design of screw piles. Job number 116394-00.

Bagheri F., El Naggar M.H. 2015. Effects of installation disturbance on behavior of multi-helix piles in structured clays. DFI Journal - The Journal of the Deep Foundations Institute, 9(2):80-91.

Basu, P., Prezzi, M. 2009. Design and applications of drilled displacement (screw) piles. Final Report FHWA/IN/JTRP- 2009/28.

Byrne, B. W., Houlsby, G.T. 2003, Foundations for offshore wind turbines. Phil. Trans. R. Soc. A 361(1813). doi:10.1098/rsta.2003.1286.

Byrne, B. W., Houlsby, G.T. 2015, Helical piles: An innovative foundation design option for offshore wind turbines. Phil. Trans. R. Soc. A 373(2035). doi:10.1098/rsta.2014.0080.

Bobbit, D.E., Clemence, S.P, 1987. Helical anchors: application and design criteria. 9th Southeast Asian Geotechnical Conference, Bangkok Thailand, 7-11 December 1987, 105-120.

CFEM. 2006. Canadian Foundation Engineering Manual. 4th Edition. Canadian Geotechnical Society, Technical Committee on Foundations, BiTech Publishers Ltd.

Chattopadhyay, B.C., Pise, P.J. 1986, Journal of Geotechnical Engineering, 112, 888-904.

Colombo, P. Colleselli, F. 1996, Elementi di Geotecnica, Zanichelli, Bologna.

Das, B.J., 1989, Uplift capacity of metal piles in clay. Proceedings of the 8th International Conference on Offshore Mechanics, Arctic Engineering, 519-524, The Hague, Netherlands.

Das, B.M. 2008. Earth Anchors. Ross, J. Publishing, Incorporated.

De Mello, J.R.C., S.R. Beim, Coelho, P.S.D., 1983. The foundation design of Campos Basin platforms. In Carneiro, F.L.L.B., Ferrante, A.J., Batista, R.C., (Eds.), Proceedings of the 4th International Symposium on Offshore Engineering, Rio de Janeiro, Brazil, pp. 112-136.

Fateh, A.M.A., A. Eslami, Fahimifar, A. 2017, Direct CPT and CPTu methods for determining bearing capacity of helical piles. Mar. Georesour. Geotech., 35(2): 193-207, http://dx.doi.org/10.1080/1064119X.2015.1133741.

Gavin, K., Igoe, D., Doherty, P. 2011, Piles for offshore wind turbines: A state of the art review. Proc. Inst. Civ. Eng. Geotech. Eng., 164, 245‑256.

Gavin, K., Doherty, P., and Tolooiyan, A. 2014. Field investigation of the axial resistance of helical piles in dense sand. Canadian Geotechnical Journal, 51(11): 1343–1354. doi:10.1139/cgj-2012-0463.

Ghaly, A.M. Hanna, A.M. 1991. Experimental and Theoretical Studies on Installation Torque of Screw Anchors" Canadian Geotechnical Journal, 28(3): 353-364.

Ghaly, A., Hanna, A., Hanna, M. 1991a. Installation Torque of Screw Anchors in Dry Sand. Soils and Foundations, 31(2), 77-92.

Ghaly, A.M., Hanna, A.M. Hanna, M.S. 1991b. Uplift Behavior of Screw Anchors in Sand -II: Hydrostatic and Flow Conditions" Journal of Geotechnical Engineering, ASCE, 117(5): 794-808.

Hoyt, R.M., Clemence, S.P. 1989. Uplift capacity of helical anchors in soil. In Proceedings of the 12th International Conference on Soil Mechanics and Foundation Engineering, Rio de Janeiro, 13–18 August 1989. A.A. Balkema, Rotterdam, the Netherlands. Vol. 2, pp. 1019–1022.

Japan Road Association 2007, Pile Foundation Design Handbook. Japan Road Association.

Jardine, R.J., Lehane, B.M., Everton, S.J. 1993. Friction coefficients for piles in sands and silts. In Offshore Site investigation and Foundation Behaviour, vol. 28, pp. 661-677, Society for Underwater Technology, 10.1007/978-94-017-2473-9_31.

Jardine, R. J., Thomsen, N.V., Mygind, M., Liingaard, M.A., Thilstead, C.L., 2015, Axial capacity design practice for North European wind-turbine projects. In Meyer, V. (Ed.), Frontiers in Offshore Geotechnics III, Boca Raton, FL: CRC Press, pp. 581‑86.

Kraft, L., Lyons, C., 1974, State of the Art: Ultimate Axial Capacity of Grouted Piles. Proceedings, Offshore Technology Conference, Houston, Texas, pp. 485-503.

Lambe, T.W., Whitman, R.V. 1969. Soil Mechanics, John Wiley & Sons.

Lehane, B.M., Schneider, J.A., and Xu, X. 2005. The UWA-05 method for prediction of axial capacity of driven piles in sand. In Frontiers in Offshore Geotechnics. Edited by Cassidy M., and Gourvenec, S. Taylor & Francis Group, London, pp. 683-688.

Livneh, B., Naggar, M.H.M., 2008. Axial testing and numerical modelling of square shaft helical piles under compressive and tensile loading. Can. Geotech.J.45(8),1142–1155.

Mitch, M.P., Clemence, S.P. 1985, The uplift capacity of helix anchors in sands. Uplift Behavior of Anchor Foundations in Soil, Detroit, Michigan, American Society of Civil Engineers, pp. 26-47.

Minnesota Department of Transportation 2007. MnDOT Pavement Design Manual.

Mittal, S., Mukherjee, S. 2013. Vertical Uplift Capacity of a Group of Helical Screw Anchors in Sand. Indian Geotechnical Journal, 43(3): 238–250.

Mitsch, M.P., Clemence, S.P. 1985. The Uplift Capacity of Helix Anchors in Sand. In Uplift Behavior of Anchor Foundations in Soil: Proceedings of a Session sponsored by the Geotechnical Engineering Division of the American Society of Civil Engineers in Conjunction with the ASCE Convention in Detroit, Mich., 24 October 1985. ASCE, New York. pp. 26–47.

Mori, G. 2003, Development of the screw steel pipe pile with toe wing, “Tsubasa Pile”. Deep Foundations on Bored and Auger Piles. In Van Impe, W.F. (Ed.) Deep Foundations on Bored and Auger Piles, Millpress, Rotterdam, pp. 171-176.

Mosquera, Z.Z., Tsuha, C.H.C., Beck, A.T. 2016. Serviceability Performance Evaluation of Helical Piles under Uplift Loading. Journal of Performance of Constructed Facilities, 30(4): 04015070.

Nagata, M., Hirata, H. 2005, Study on the uplift resistance of screwed steel pile. Nippon Steel Technical Report, N. 92, 73-78.

Newgard, J.T., Schneider, J.A., and Thompson, D.J. 2015. Cyclic response of shallow helical anchors in a medium dense sand. In Frontiers in Offshore Geotechnics III. Edited by V. Meyer. Taylor & Francis Group, London, pp. 913-918.

NSENGI, 2013, ECO Pile. http://www.nsec-steelstructures.jp/data/ns_ecopile/ (last access November 14, 2018).

Peck, R., Hanson, W., Thornburn, T. 1974. Foundation Engineering Handbook. Wiley, London.

Perko, H.A. 2000. Energy Method for Predicting the Installation Torque of Helical Foundations and Anchors. New Technological and Design Developments in Deep Foundations, ASCE.

Perko, H.A., 2009, Helical Piles. John Wiley & Sons, Inc. Hoboken, New Jersey.

Poulos, H.G., 1988, Marine Geotechnics. Spon Press.

Randolph, M., Cassidy, M., Gourvenec, S., Erbrich, C., 2005, Challenges of Offshore Geotechnical Engineering. 16th Int. Conf. on Soil Mechanics and Geotechnical Engineering, Osaka, September 2005, IOS Press, pp. 123 – 176.

Randolph, M., Gourvenec, S., 2011, Offshore Geotechnical Engineering, Spon Press, Oxon.

Rao, S. N., Prasad, Y., Shetty, M. D. 1991. The behaviour of model screw piles in cohesive soils. Soils and Foundations 31(2):35–50. doi:10.3208/sandf1972.31.2_35.

Saeki, E., Ohki, H. 2003, A study of the screwed pile- the results of installation and loading tests and analysis of penetration mechanism. In Van Impe, W.F. (Ed.) Deep Foundations on Bored and Auger Piles, Millpress, Rotterdam, pp. 259-266.

Saeki E., Ohki, H. 2000. A study of the screwed pile-the results of installation and loading tests and analysis of penetration mechanisms. Nippon Steel Technical Report 82, 42-50.

Sakr, M. 2009, Performance of helical piles in oil sand. Can. Geotech. J., 46(9): 1046-1061.

Sakr, M. 2015. Relationship between Installation Torque and Axial Capacities of Helical Piles in Cohesive Soils. The Journal of Performance of Constructed Facilities.

Son, L.M., 2002, Compiling geotechnical data to determine the distribution and properties of top sand deposits in quadrant K &L of the Dutch sector-North Sea. Master thesis, Delft University of Technology.

Schiavon, J.A., Tsuha, C.H.C., Neel, A., Thorel L. 2016. Physical modelling of a single-helix anchor in sand under cyclic loading. In Proceedings of 3rd European Conference on Physical Modelling in Geotechnics Eurofuge 2016, 1-3 June 2016, Nantes, France.

Schiavon, J. A. 2016. Behaviour of helical anchors subjected to cyclic loadings. PhD thesis, University of São Paulo, São Carlos, SP, Brazil.

Schiavon, J.A., Tsuha, C.H.C., Thorel L., 2017. Cyclic and post-cyclic monotonic response of a single-helix anchor in sand. Geotechnique Letters, 7(1), 11-17.

Spagnoli G. 2013. Some considerations regarding the use of helical piles as foundation for offshore structures. Soil Mechanics and Foundation Engineering 50(3): 102-110, DOI: 10.1007/s11204-013-9219-7.

Spagnoli G., Mendez C.M., Tsuha, C.H.C., Oreste P. In review. A parametric analysis for the estimation of the installation power for helical piles in cohesionless soils.

Spagnoli G., Tsuha, C.H.C., Oreste P., Mendez C.M. In review. Estimation of uplift capacity and installation power of helical piles in sand for offshore structure.

Spagnoli, G., Gavin, K., Brangan, C., Bauer, S. 2015. In situ and laboratory tests in dense sand investigating the helix-to-shaft ratio of helical piles as a novel offshore foundation system. In Frontiers in Offshore Geotechnics III. Edited by V. Meyer. Taylor & Francis Group, London, pp. 643-648.

Spagnoli, G., Gavin, K. 2015. Helical Piles as a Novel Foundation System for Offshore Piled Facilities. In Abu Dhabi International Petroleum Exhibition and Conference, 9-12 November, Abu Dhabi, UAE, https://doi.org/10.2118/177604-MS.

Spagnoli, G. 2017. A CPT based-model to predict the installation torque of helical piles in sand. Marine Georesources & Geotechnology, 35(4): 578-585.

Spagnoli, G., 2017, A CPT-based model to predict the installation torque of helical piles in sand. Mar. Georesour. Geotech., 35(4), 578-585, DOI: 10.1080/1064119X.2016.1213337.

Steel Construction Manual, 1986, American Institute of Steel Construction, Chicago.

Tadashi, M., Mikio, F., 2009. A study on end-bearing capacity mechanism of steel spiral pile. In Deep Foundations on Bored and Auger Piles. In Van Impe, W.F., Van Impe, P.O. (Eds.), Proceedings of the 5th International Geotechnical Seminar on Bored and Auger Piles, London: Taylor and Francis Group, pp. 161-166.

Trofimenkov, J. G., Mariupolskii, L.G., 1965. Screw Piles Used for Mast and Tower Foundations. Proceedings of 6th International Conference on Soil Mechanics and Foundation Engineering, Montreal, Quebec, Vol. 11, pp. 328-332.

Tsuha, C.H.C. 2007. Theoretical model to control on site the uplift capacity of helical screw piles embedded in sandy soil. Ph.D. thesis, Department of Geotechnics, Sao Carlos School of Engineering, University of Sao Paulo, Sao Carlos, Brazil.

Tsuha, C.H.C., Aoki, N. 2010. Relationship between installation torque and uplift capacity of deep helical piles in sand. Canadian Geotechnical Journal, 47(6): 635–647, 10.1139/T09-128.

Vesic, A.S. 1971. Breakout resistance of objects embedded in ocean bottom. Journal of the Soil Mechanics and Foundations Division ASCE, 97(9): 1183–1205.

Wada, M., Tokimatsu, K., Maruyama, S., Sawaishi, M., 2017. Effects of cyclic vertical loading on bearing and pullout capacities of piles with continuous helix wing. Soils Found., 57: 141–153, http://dx.doi.org/10.1016/j.sandf.2017.01.010.

Weech, C. N., Howie, J. A. 2012. Helical piles in soft sensitive soils–a field study of disturbance effects on pile capacity. VGS Symposium on Soft Ground Engineering.

Wu, T.H., Lee, I.M., Potter, J.C., Kjekstad, O., 1987. Uncertainties in Evaluation of Strength of Marine Sand. Journal of Geotechnical Engineering 113(7), 719-738.

Young, A.G., Sullivan, R.A., 1978. Pile design and installation features of the Thistle platform. European Offshore Petroleum Conference and Exhibition, London 24-27 October, 1978, 101-110, https://doi.org/10.2118/8050-MS.

Zhang, D.J.Y. 1999. Predicting capacity of helical screw piles in Alberta soils. Master thesis, Department of Civil and Environmental Engineering, University of Alberta, Edmonton, Alta.